



The radiation yield in different spectral ranges from low density structured laser plasma with different high z-admixture

V. Rozanov

P.N. Lebedev Physical Institute of RAS, Moscow, Russia

E-mail: rozanov@sci.lebedev.ru



Topics

- Laser plasma - Radiation source**
- Energy balance: main processes**
- Radiation sources: ICF physics (hohlraum), diagnostics, material sciences, technology - EUV lithography source**
- Requirements: target designs**
- Experimental results**
- Theoretical models and simulation**
- Conclusion**

Abstract



channeling ZVIII

V.B.Rozanov P.N Lebedev Institute

25/10 - 1/11/2008, Erice (Trapani - Sicily), Italy



The laser radiation has low entropy, and, thus, may be effectively converted into the radiation of a more hard range. The problem is to find particular schemes for different tasks. The competing processes under the laser plasma heating are the plasma thermal radiation and the plasma expansion - the conversion of the laser pulse energy into the plasma kinetic energy. The efficiency of the two mentioned processes depends on the density and size of plasma, and may be effectively controlled by these two parameters: a decrease of density and an increase of the target size enhance the efficiency of radiation. The radiation spectrum depends on the plasma composition and the heavy admixtures concentration in the plasma. In the last two years in laser irradiation of the target researches the scientists have been deeply involved in studying of the energy transformation and transfer (including the radiation) processes in low-density structured foam-like media with an addition of different (in particular, heavy) elements.

It has been found experimentally that under laser irradiation of a foam-line target with the heavy ion admixture it is possible to produce the radiation with the efficiency close to 50%.

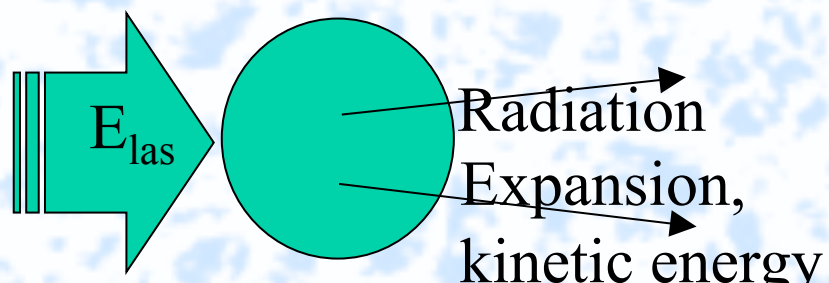
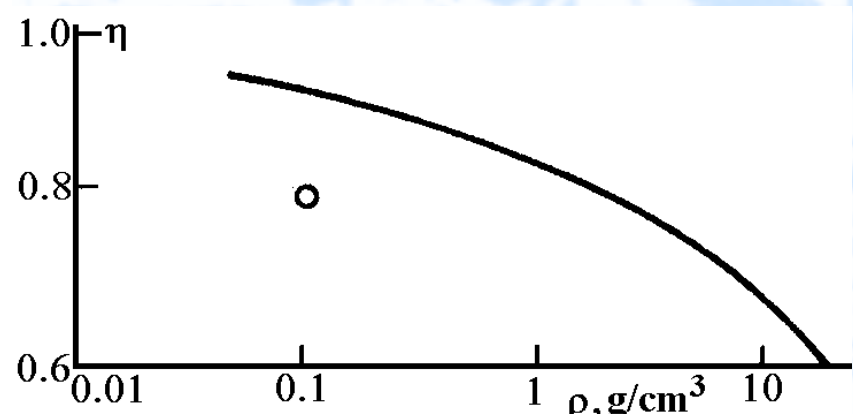
This report concerns a theoretical basis and the experimental results related to the problem.

Effective Conversion of Laser Radiation into Plasma Self-emission

(G.A.Vergunova, V.B.Rozanov, Kvantovaya Elektronika, v.19, N3. 263-265, 1992)



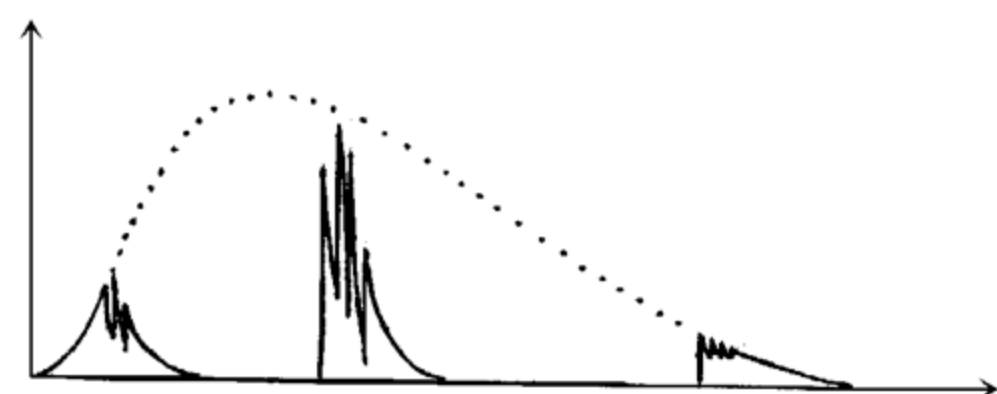
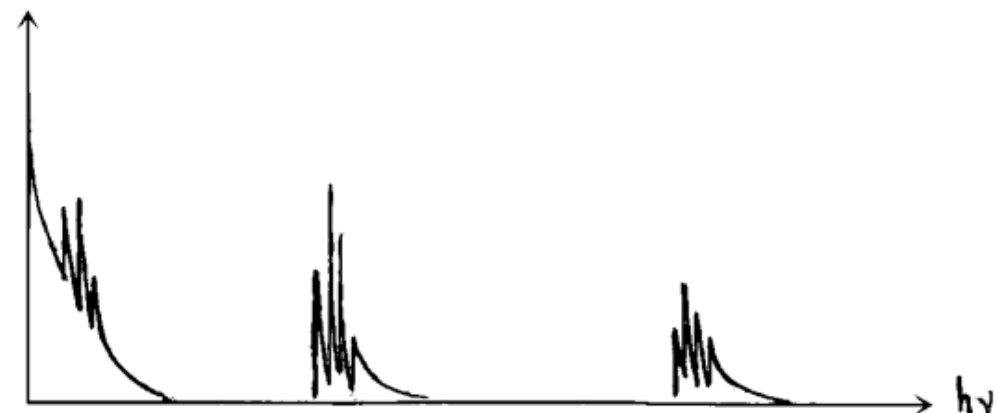
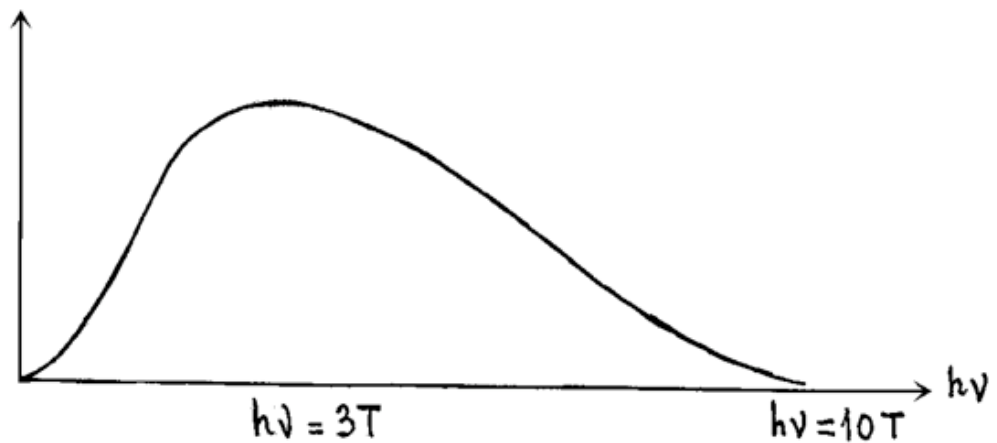
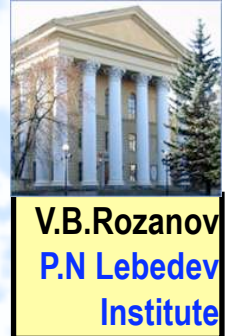
Target density influence
Optic-transparent plasma



Coefficient of laser radiation conversion in plasma self-emission,
 $\lambda=1.06\mu\text{m}$, $\tau=4\text{ns}$, $q_{\text{las}}=10^{13} \text{ W/cm}^2$.
 $E_{\text{las}} = N\varepsilon = 4\pi R^2 q_{\text{las}} \tau_{\text{las}} = 4\pi R^3/3 \cdot n\varepsilon$,
N - total number of particles in the target, ε - energy per particle,
 $\tau_{\text{rad}} = n\varepsilon/j$, j - emissivity, n - density
 $\tau_{\text{exp}} = R/c_s$, R - target radius, c_s - sound velocity

High efficiency radiation conversion condition: $\tau_{\text{rad}} < \tau_{\text{exp}}$
or $jR/c_s \sim \varepsilon n$

K-electrons radiation (1)



Low entropy laser radiation:

$$dE_{\text{las}} = T dS$$

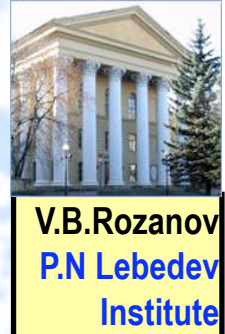
dS is small,

$T \sim h\nu$ is high

Black body radiation:

$$S_{v,\text{eq}} = \frac{2\pi h\nu^3}{c^2} \frac{\nu^3}{\exp\left(\frac{h\nu}{kT}\right) - 1}$$

K-electrons radiation (2)



Atoms	Ti	Cu	Ge	Kr	Zr	Ag
Z	22	29	32	36	40	47
hν, keV	6.6	11.3	13.8	17.6	21.8	30

Emissivity of the plasma (Bremsstrahlung + photorecombination):

$$J = 4.85 \cdot 10^4 \bar{z} z^2 n_i^2 T_e^{1/2} (2.4 I_e/T_e + 1) \frac{\text{erg}}{\text{cm}^3 \text{s}} , \quad T_e - \text{keV}$$

Opacity: $J = \int j_v dv$ $j_v = \kappa_v I_{v,eq}$ $I_{v,eq}$ - black BR intensity

K-electrons radiation (3)



V.B.Rozanov
P.N Lebedev
Institute

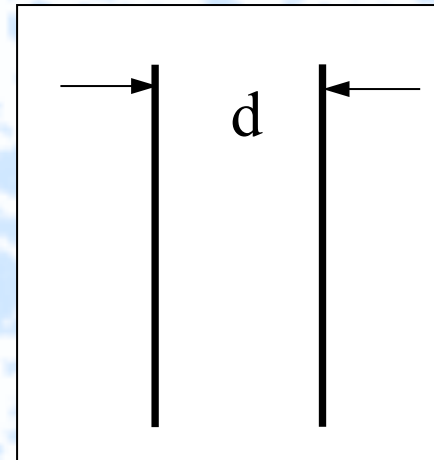
Plane target:

$$\tau_v = d/l_v = \kappa_v - \text{optical thickness}$$

Photons escape probability:

$$W_v^{(1)} = \frac{1}{\tau_v} \left[\frac{1}{2} - \int_1^{\infty} \exp(-x\tau_v) \frac{dx}{x^3} \right]$$

$$S_v^{(1)} = 4\pi j_v W_v^{(1)} \frac{d}{2} = \pi l_{v,\text{eq}} [1 - 2E_3(\tau_v)]$$



Spherical target:

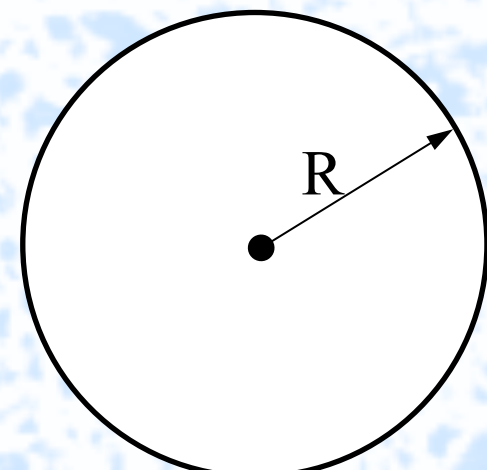
$$x_v = 2R/l_v = \kappa_v 2R - \text{optical thickness}$$

Photons escape probability:

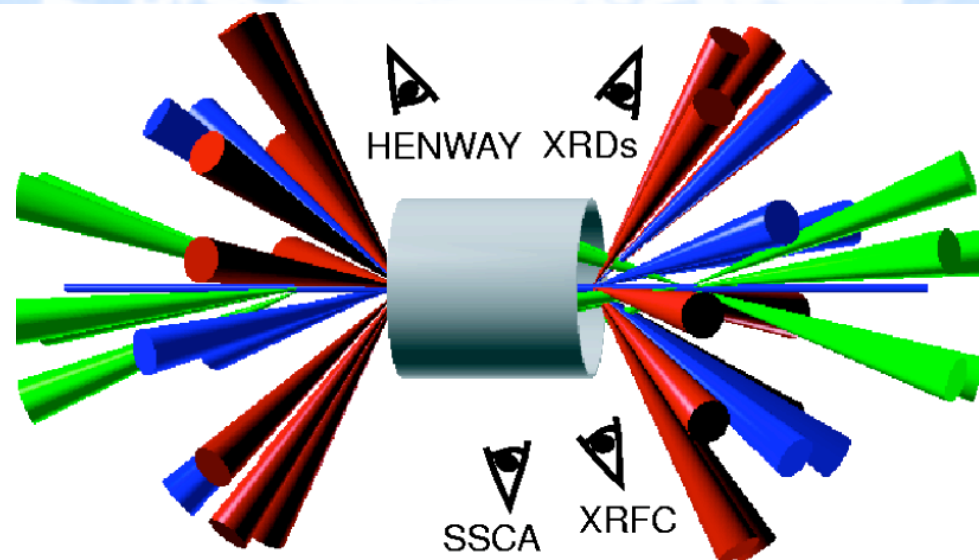
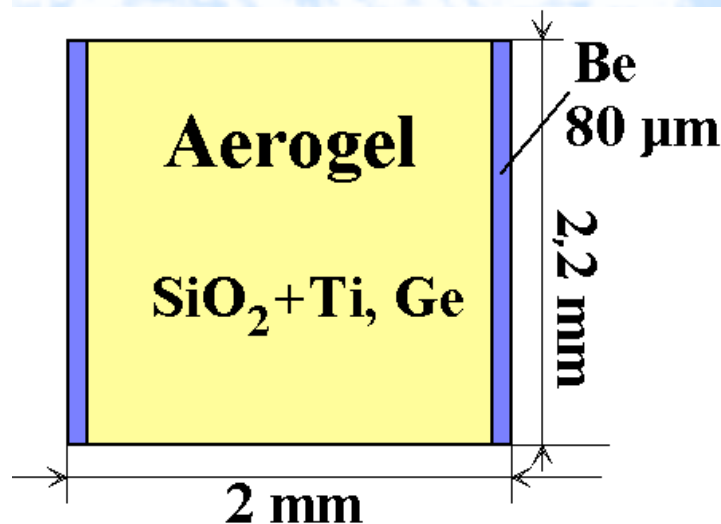
$$W_v^{(3)} = \frac{3}{x_v} \left[\frac{1}{2} - \frac{1}{x_v} \left(\frac{1}{x_v} - \left[1 + \frac{1}{x_v} \right] e^{-x_v} \right) \right]$$

$$S_v^{(3)} = 4\pi j_v W_v^{(3)} \frac{R}{3} \quad \underline{\text{If } R = 1.4d}$$

$$\frac{|S_v^{(1)} - S_v^{(3)}|}{S_v^{(1)}} < 7\%$$



K-electrons radiation (4)



$$E_L = 7 - 14 - 20 \text{ kJ}, \quad 3\omega, \quad \tau_L = 1 \text{ ns (square form)}$$

$$I_L = (1.7 - 8)10^{15} \cdot \text{W/cm}^2 \text{ (Omega laser, LLE)}$$

Aerogel: $\rho = (3.1 - 6.5) \text{ mg/cm}^3$

Ti at. 3% Ge at. <20%

Ti: $4.67 < h\nu < 5 \text{ keV}$ Output $1.9\% \cdot 14.5 \text{ kJ} = 290 \text{ J}$

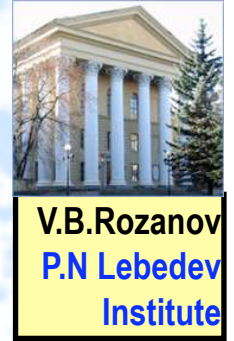
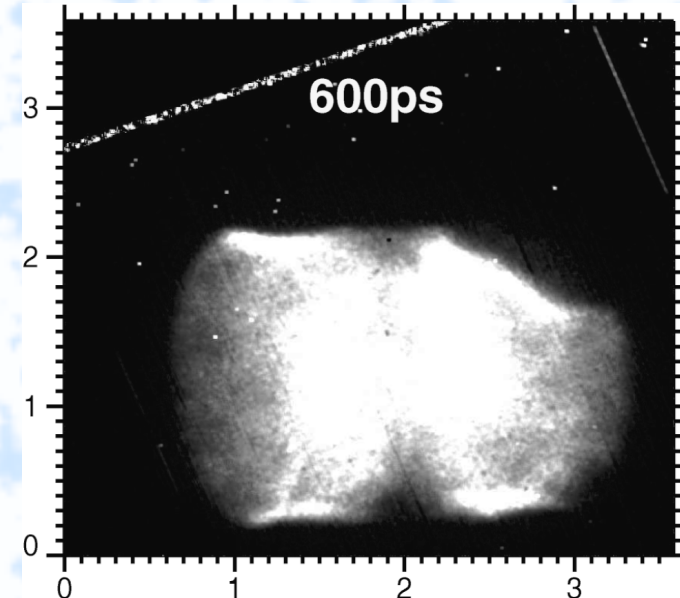
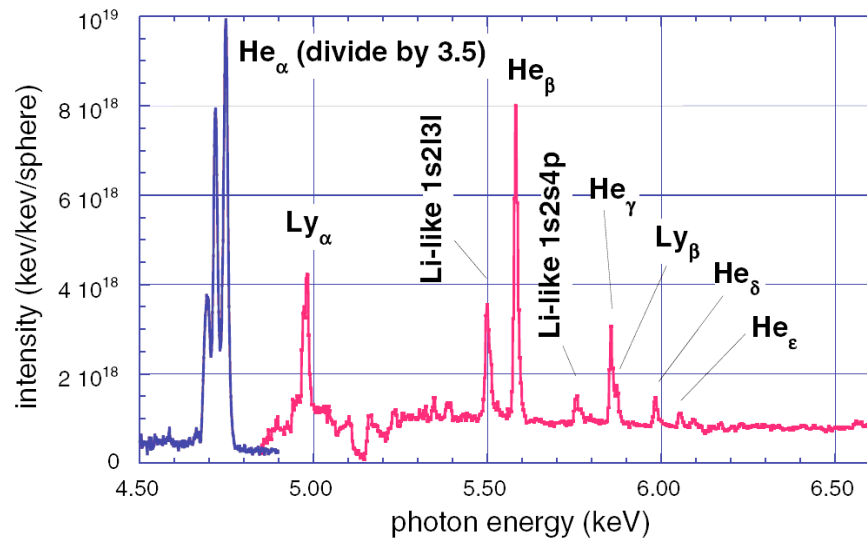
Ge: $10 < h\nu < 13 \text{ keV}$ Output $1 - 3\% \cdot 20 \text{ kJ} = 200 - 600 \text{ J}$
 $h\nu < 2 \text{ keV}$ Output $\sim 50\% \approx 10 \text{ kJ}$

* M.Tobin et al., ECLIM 29, 2006, Madrid, Spain

* K. Fournier et al., Phys.Rev.Lett., v.92, 165005 (2004)

K-electrons radiation (5)

Ti K-shell spectrum



$$E_L = 7 - 14 - 20 \text{ kJ}, \quad 3\omega, \quad \tau_L = 1 \text{ ns (square form)}$$

$$I_L = (1.7 - 8)10^{15} \cdot \text{W/cm}^2 \text{ (Omega laser, LLE)}$$

Aerogel: $\rho = (3.1 - 6.5) \text{ mg/cm}^3$

Ti at. 3% Ge at. <20%

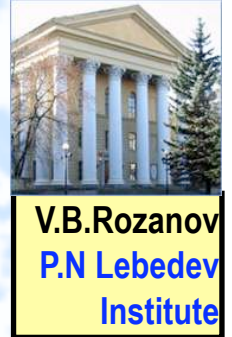
Ti: $4.67 < h\nu < 5 \text{ keV}$ Output $1.9\% \cdot 14.5 \text{ kJ} = 290 \text{ J}$

Ge: $10 < h\nu < 13 \text{ keV}$ Output $1 - 3\% \cdot 20 \text{ kJ} = 200 - 600 \text{ J}$
 $h\nu < 2 \text{ keV}$ Output $\sim 50\% \approx 10 \text{ kJ}$

* M.Tobin et al., ECLIM 29, 2006, Madrid, Spain

* K. Fournier et al., Phys.Rev.Lett., v.92, 165005 (2004)

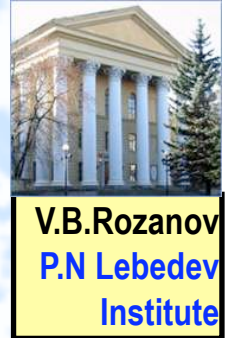
Requirements for properties of the radiation sources



**Soft x-ray source for scientific investigation
and technology application (including biological
objects investigation and material sciences):**

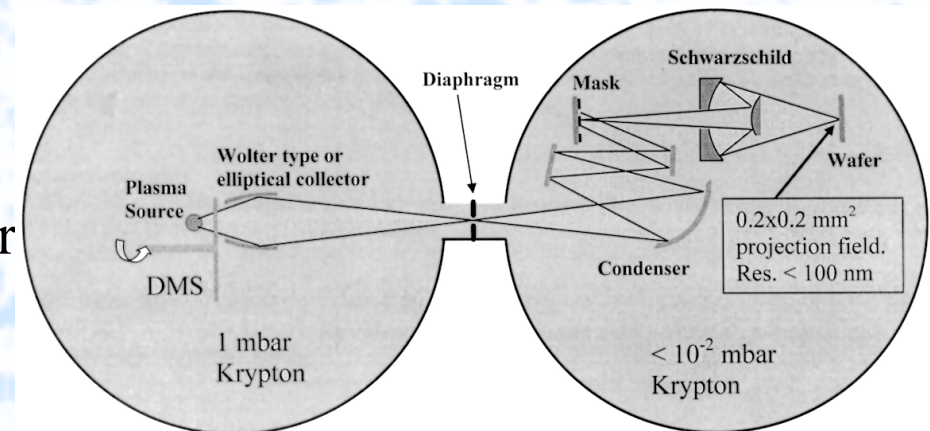
- Spectral range $h\nu \sim 50\text{eV} - 20\text{ keV}$
- High efficiency
- Single shot and repetition rate modes
- Stable, efficient and clean source
- Soft x-ray source requirements (LPI, TRINITI)

Requirements for properties of the radiation sources

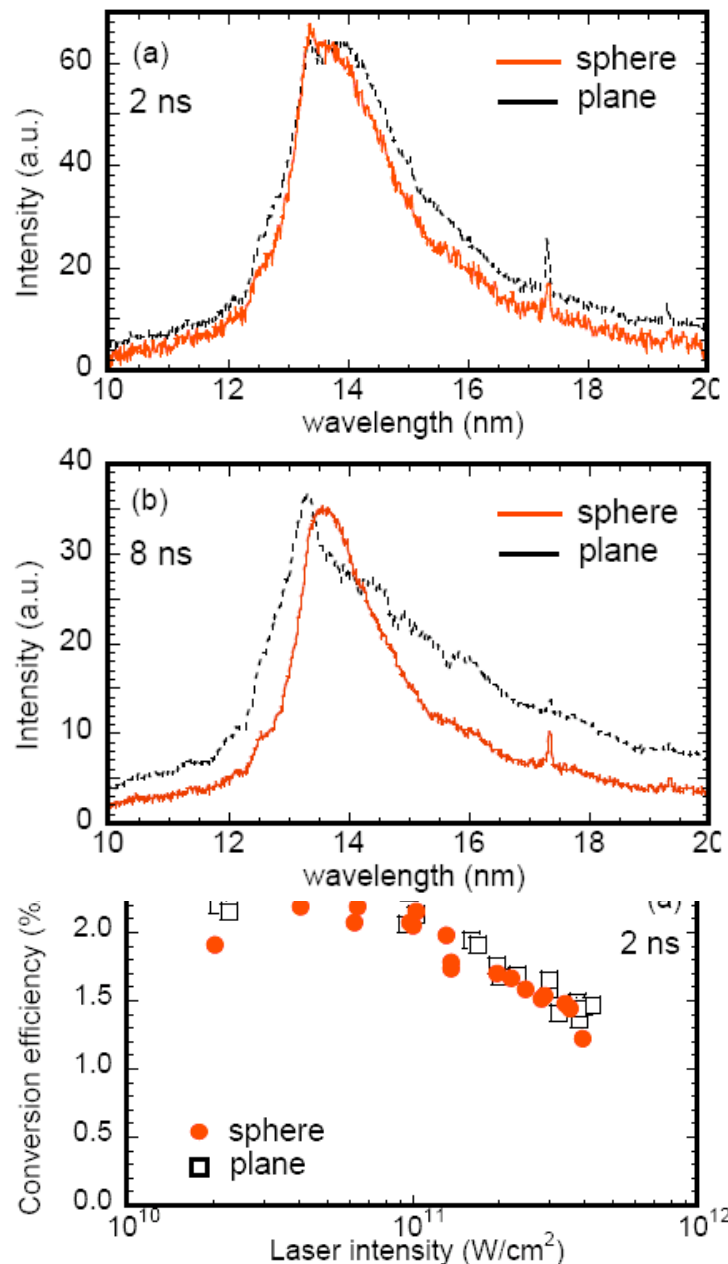


EUV lithography source:

- Spectral range 13 - 14 nm
- Repetition rate mode. Average power P_{hv} in the intermediate focus in the 2% bandwidth around 13.5 nm - 100W
- Efficiency in the useful band $\sim 2\%$
- Lifetime of optic system about ~ 1 year
- Debris mitigation problem
- EUVL prototype of the FIRB project (ENEA, Frascati, S.Bollanti, F.Flora et al)



EUV-source



Requirement:

100 W, 30000 hours lifetime

Single shot:

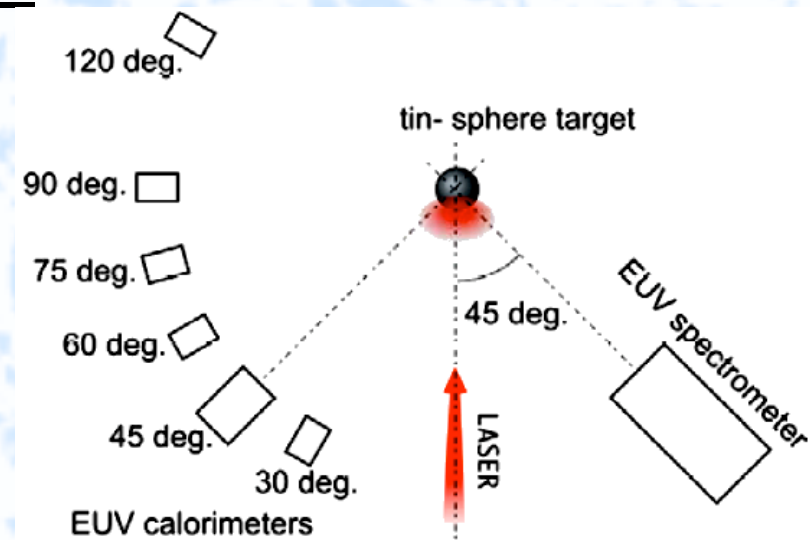
$\tau_L = 2 \text{ and } 8 \text{ ns}$

$I_L = 10^{10} - 5 \cdot 10^{11} \text{ W/cm}^2$

$\eta \approx 2\%$

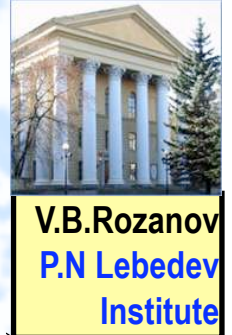
Rep. rate 10 Hz

$\eta \approx 0.2\%$

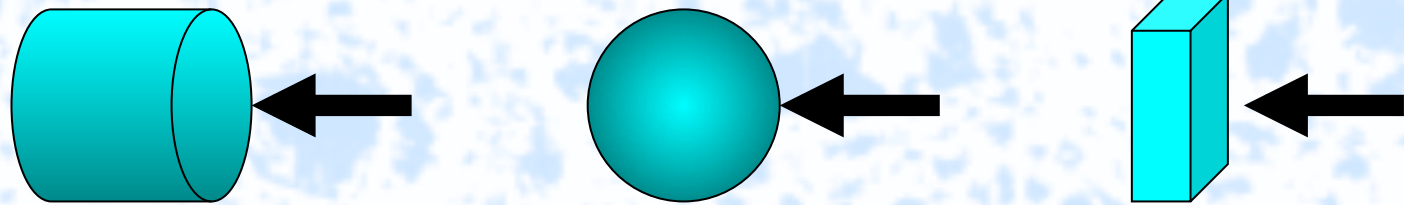


Experimental arrangement.

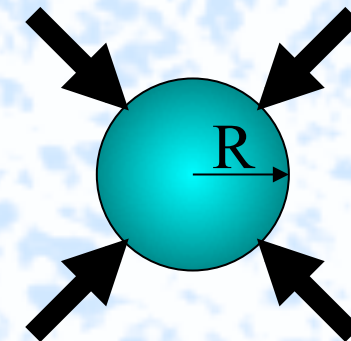
Target physics. Main Relations⁽¹⁾



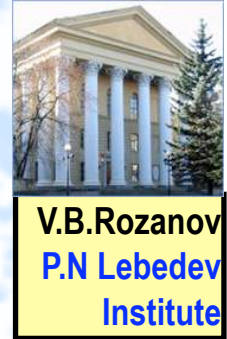
- We will use one-side irradiation of cylindrical (spherical, plane) target.



- Simple model: Spherical target,
Symmetrical irradiation
- $P_L = E_L v$, v - repetition rate, single shot - E_L
- $E_L = 4\pi R^2 q_L \tau_L$, $E_L = N\epsilon$, q_L - laser intensity, τ_L - laser pulse duration
- $N = R^3 n \cdot 4\pi/3$ - total number of atoms in the target, n - particles density
- $\epsilon = \epsilon_T + \epsilon_{ion} + \epsilon_{kin}$ - energy per particle

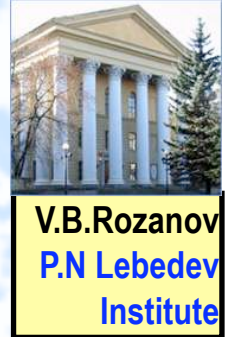


Target physics. Main Relations⁽²⁾



- $\kappa R \geq 1$ Laser radiation absorption condition
- $\tau_{\text{exp}} = R/c_s$, c_s - sound velocity, τ_{exp} - time of expansion, transition of laser energy into kinetic energy
- $\tau_{\text{rad}} = n\varepsilon/j$, j - emissivity ($\text{erg} \cdot \text{cm}^3/\text{s}$) integrated over spectrum, τ_{rad} - time of the laser energy transition into radiation energy
- $\tau_{\text{rad}} < \tau_{\text{exp}}$ Condition of high efficiency of radiation
- $j \tau_{\text{exp}} / (n\varepsilon) = \eta_{\text{rad}}$ - efficiency of radiation
- Spectral range of radiation depends on the spectral emissivity $j(hv)$, density n and plasma temperature T

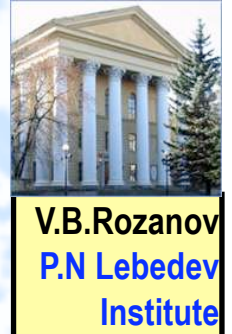
Target physics. Main Relations⁽³⁾



Important parameters of the problem:

- $P, E_L, v, q_L, \tau_L, \varepsilon, \tau_{rad}, \tau_{exp}, n, T, j = \int j(hv)dhv$
- Examples: $P_{hv} = 100W, \eta_{hv} = 2\%, P_L = 5 \cdot 10^3 W = E_L v,$
 $v=100, E_l = 50J \quad - OR - \quad v=10000, E_l = 0.5J$
- What is better for high efficiency? There are wide fields for optimization between parameters indicated above.

- The targets made of low density foams with heavy elements dopants (clusters) give good possibilities to choose appropriate condition for high efficiency laser energy transformation into radiation energy in EUV of soft x-ray ranges.
- The foam targets have additional possibilities to solve the debris problem

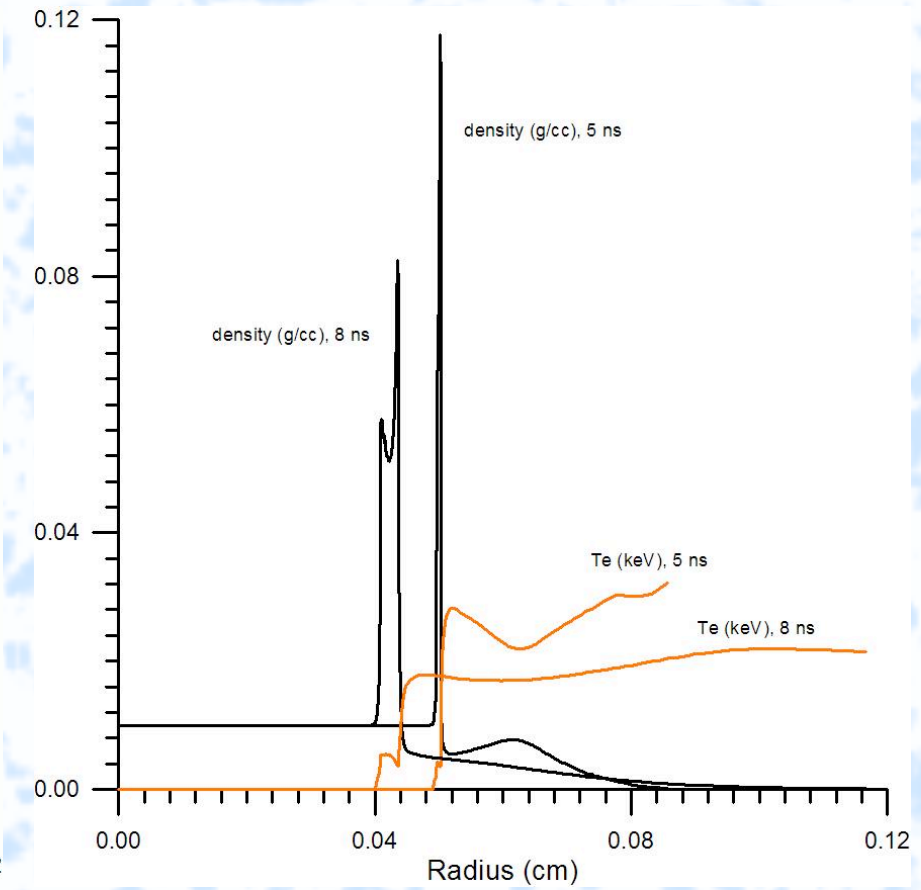
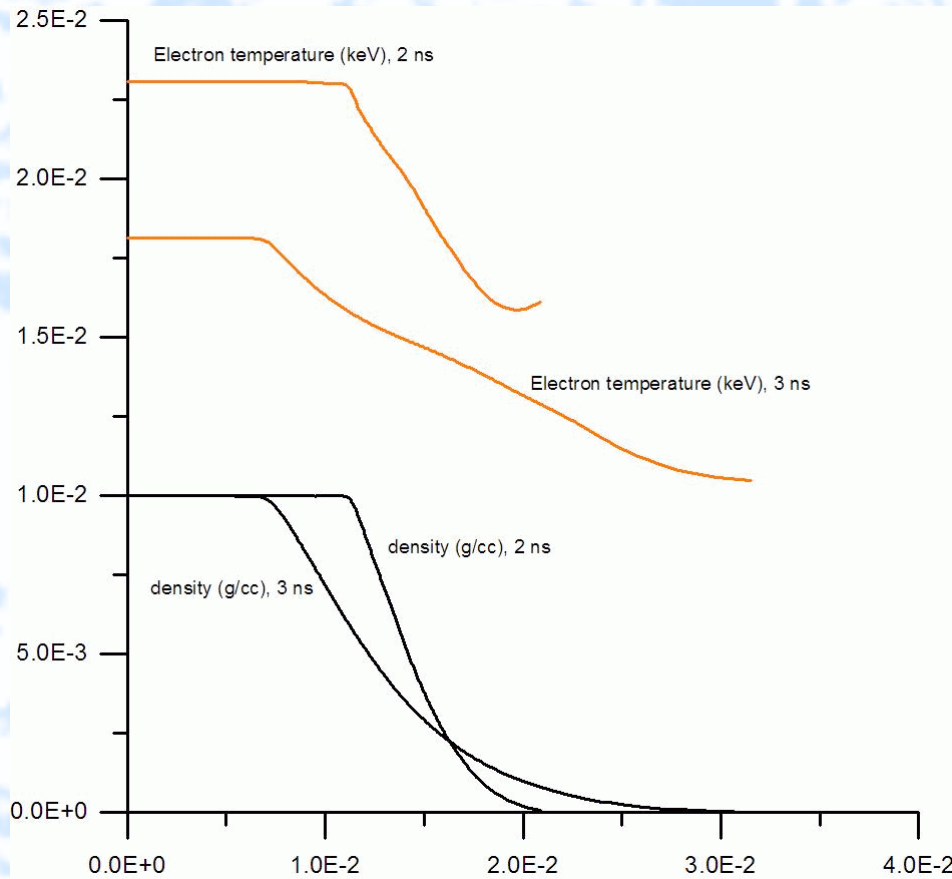


Simulation DIANA 1D

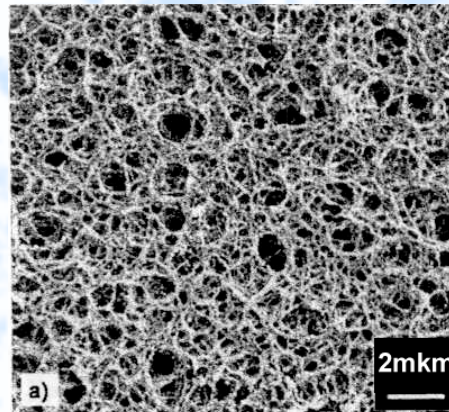
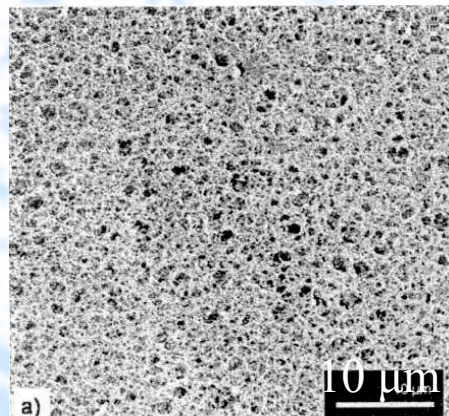
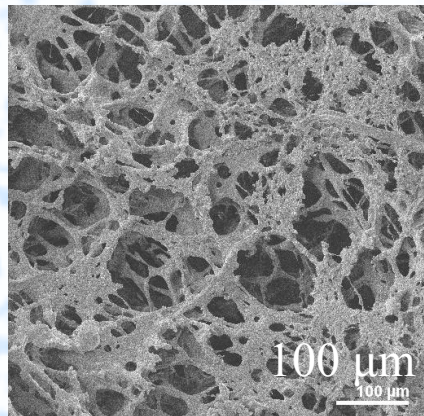
Homogeneous media (LPI, IMM, 2006)

$$E_L = 0.5 \text{ J} \quad I_L = 10^{11} \text{ W/cm}^2 \\ E_R = 23\%$$

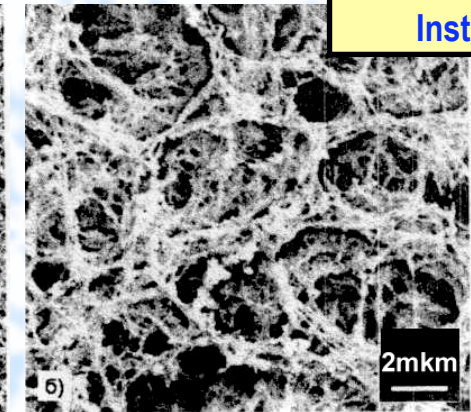
$$E_L = 50 \text{ J} \quad I_L = 10^{11} \text{ W/cm}^2 \\ E_R = 53\%$$



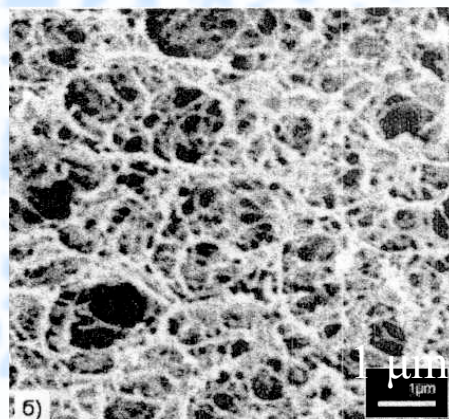
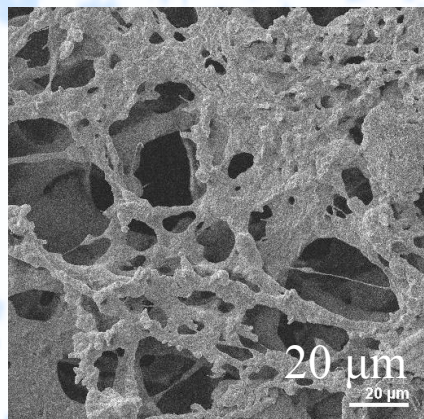
Foams



TAC
 $9.1\text{mg}/\text{cm}^3$

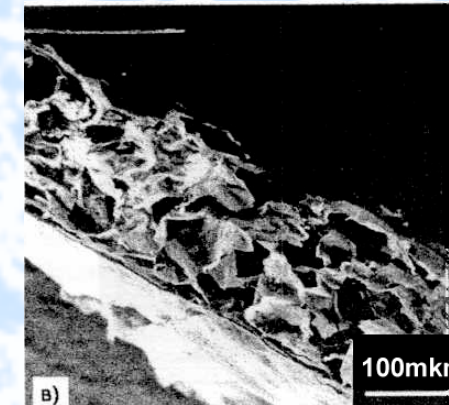


TAC + 9.9%Cu
 $9.1\text{mg}/\text{cm}^3$

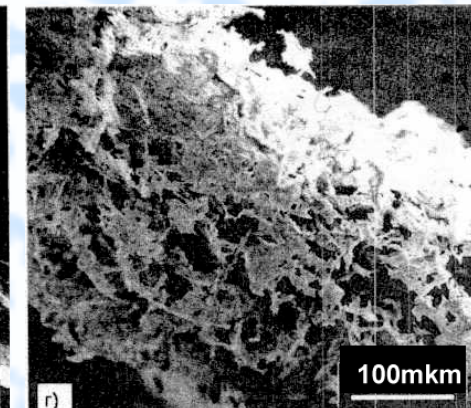


Polystyrene
+NaCl

TAC $4.5\text{mg}/\text{cm}^3$

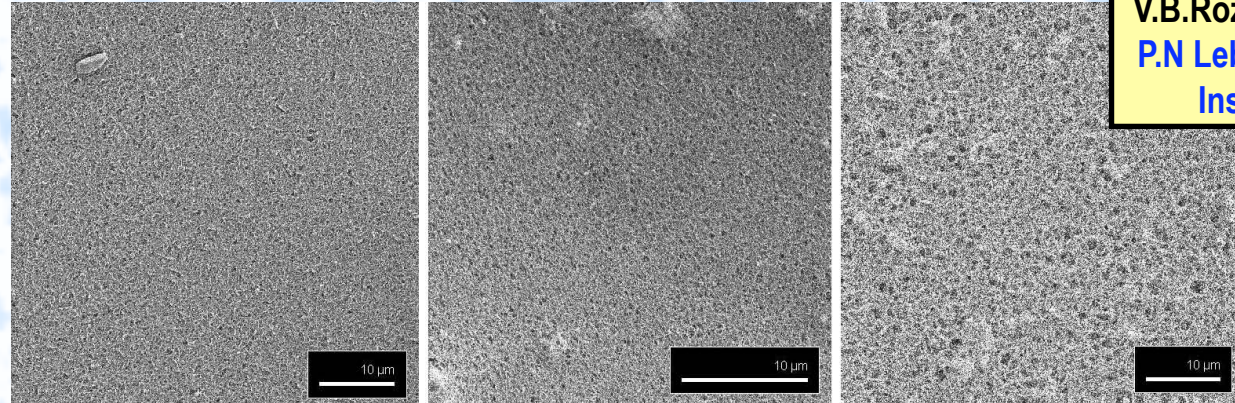
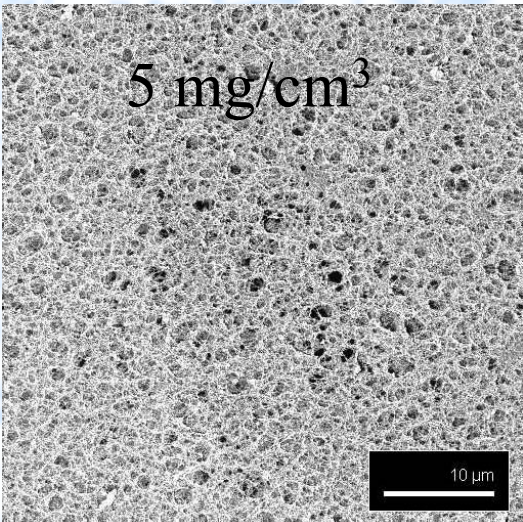


agar
 $20\text{mg}/\text{cm}^3$

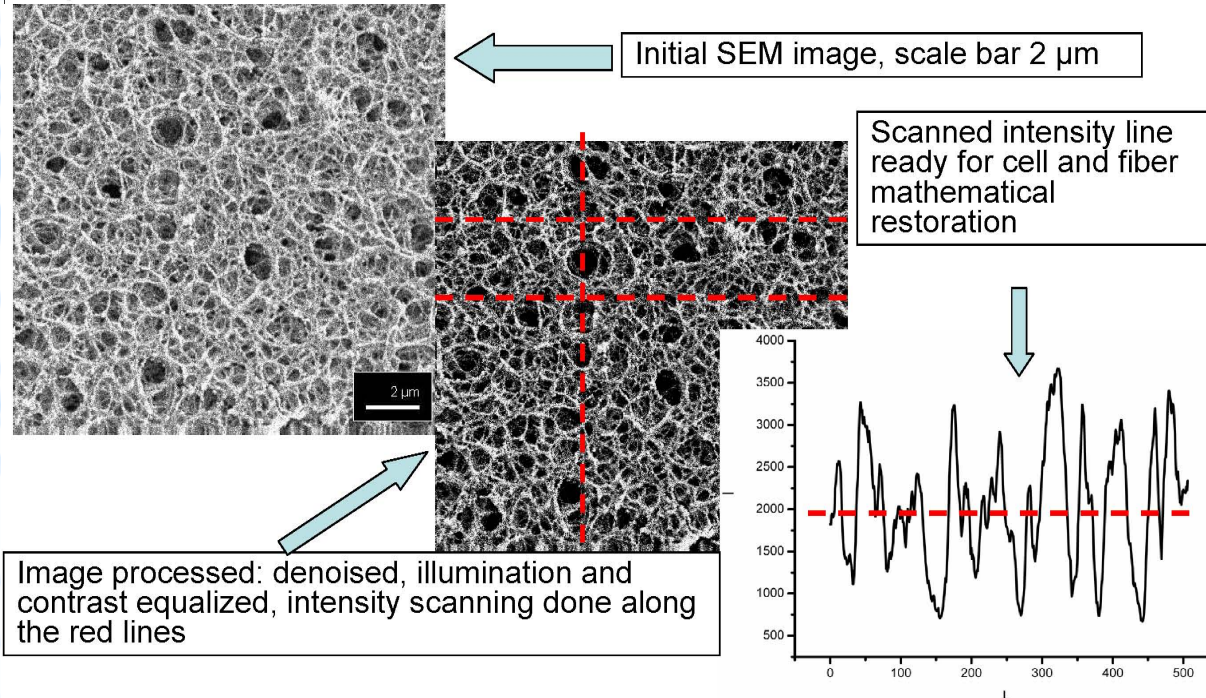


agar $10\text{mg}/\text{cm}^3+$
 $\text{SnO}_2 10\text{mg}/\text{cm}^3$

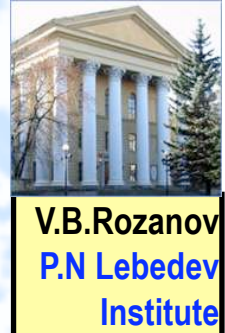
TAC foam structure



TAC structure of 10 mg/cc (SEM) from left to right: without Cu, with Cu nanoparticles of 10% by weight and of 20% by weight. Scale – 10 µm. Synthesis in IOCh 01/19/2005



Foam parameters



PALS : TAC - $C_{12}H_{18}O_8$

$\lambda_{1\omega} = 1.315 \mu\text{m}$, $N_{e\text{ cr }1\omega} = 0.6 \cdot 10^{21} \text{ 1/cc}$	$\lambda_{3\omega} = 0.438 \mu\text{m}$, $N_{e\text{ cr }3\omega} = 5.4 \cdot 10^{21} \text{ 1/cc}$
---	---

Targets: TAC on 5 μm Al

$$\rho_1 = 4.5 \mu\text{g/cc};$$

$$\rho_2 = 9.1 \mu\text{g/cc};$$

$$\rho_3 = 9.1 \mu\text{g/cc} - \text{TAC} + 9.9\% \text{ Cu}$$

For $\lambda_{1\omega}$ TAC targets are overcritical:

For $\lambda_{3\omega}$ TAC targets are undercritical:

LIL: TMPTA - $C_{15}H_{20}O_6$

$\lambda_{1\omega} = 1.05 \mu\text{m}$, $N_{e\text{ cr }1\omega} = 1021 \text{ 1/cc}$	$\lambda_{3\omega} = 0.351 \mu\text{m}$, $N_{e\text{ cr }3\omega} = 9 \cdot 1021 \text{ 1/cc}$
---	--

TMPTA foam 900 μm 6.5 $\mu\text{g/cc}$

For $\lambda_{3\omega}$ TMPTA targets are undercritical

- A.M. Khalenkov, N.G. Borisenko, et al. Experience of microheterogeneous target fabrication to study energy transport in plasma near critical density. // Laser & Particle Beams, 2006, **24**, pp. 283-290.

- N.G. Borisenko, et al. Regular 3D networks with clusters for controlled energy transport studies in laser plasma near critical density. // Fusion Sciences and Technology, 2006, **49**, #4, pp. 676-685.

- N.G. Borisenko, et al. Intensive (up to 1015W/cm²) Laser Light Absorption and Energy Transfer in Subcritical Media with or without High-Z Dopants. AIP Conference Proceedings, 2006, **849**, pp. 242-246/

Radiative characteristics of different plasmas for radiation near 13-14 nm: Xe,Sn,O ... (1)

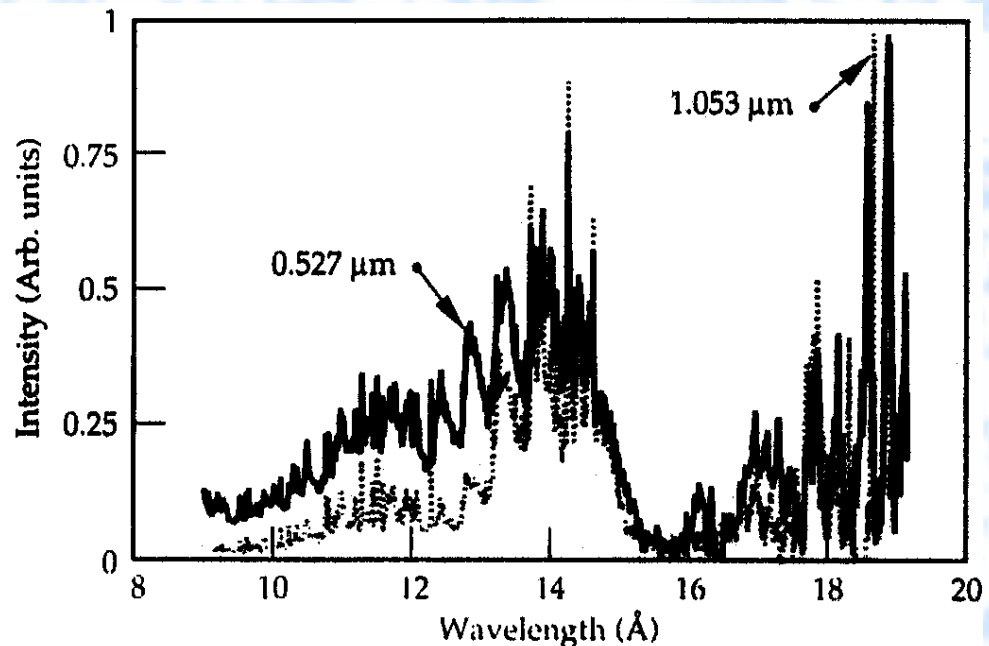
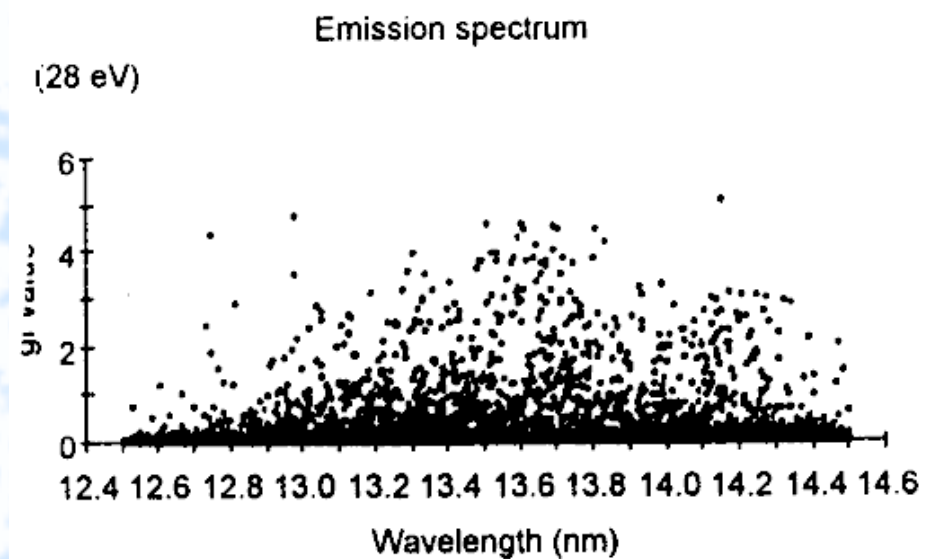


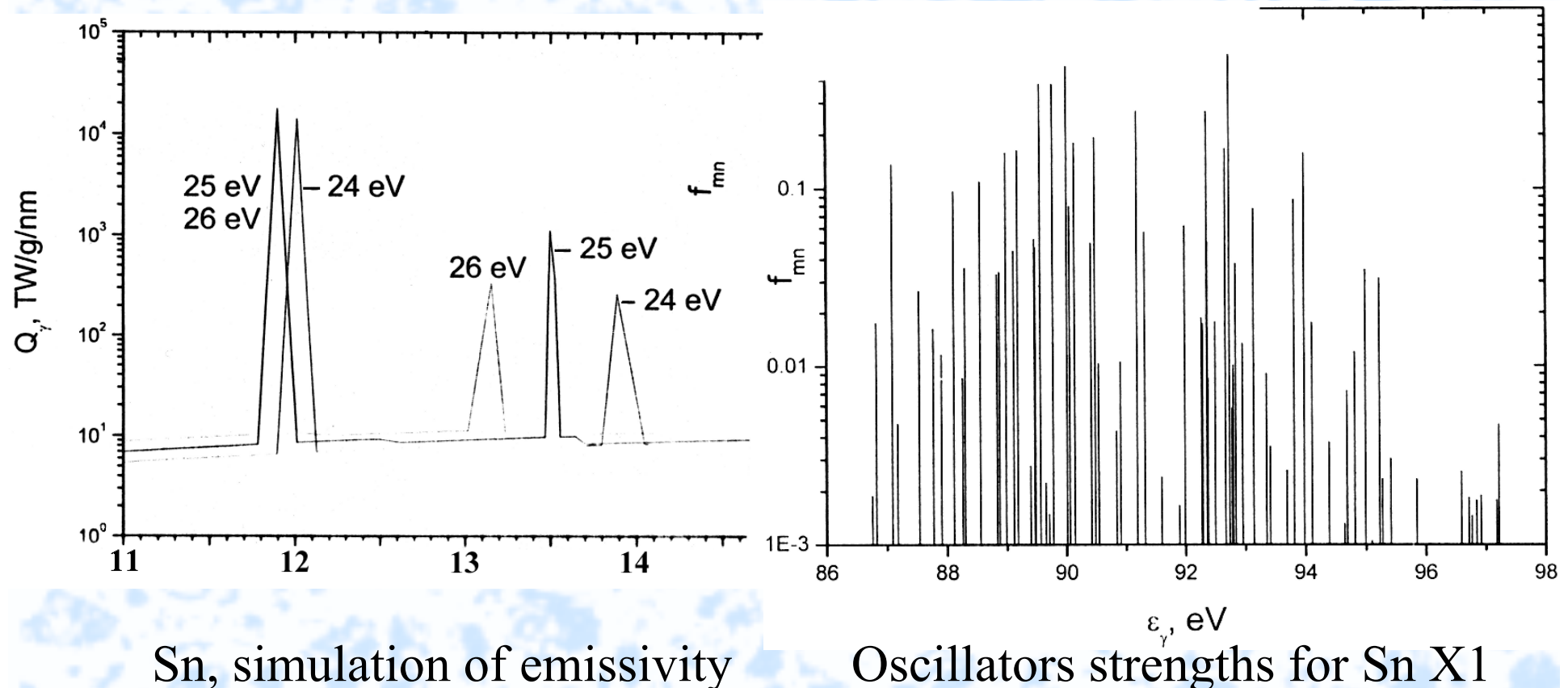
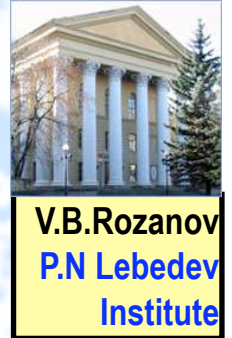
FIGURE 9. Comparison of x-ray spectra from solid Xe measured from plasmas produced with 1.053- μm (dashed line) and 0.527- μm (solid line) laser light. (20-07-0695-1659pb01)

Solid Xe experiments, 1995 (UCRL)



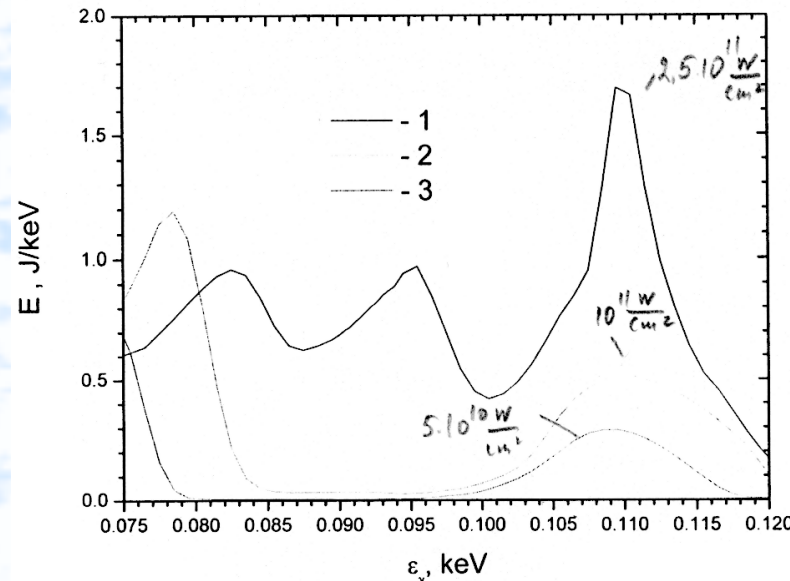
Sn, T=28 eV simulation,
2003 (Dublin Univ.)

Radiative characteristics of different plasmas for radiation near 13-14 nm: Xe,Sn,O ... (2)

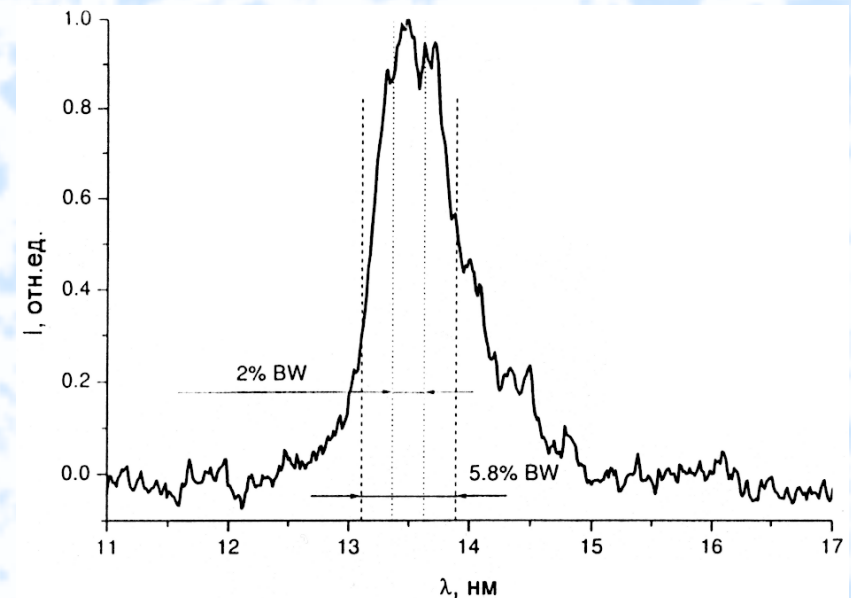


RFNC-VNIIEF, Sarov, 2006

Radiative characteristics of different plasmas for radiation near 13-14 nm: Xe,Sn,O ... (3)

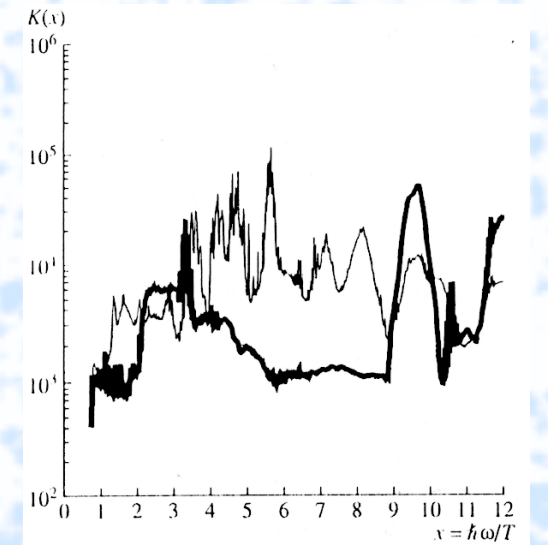
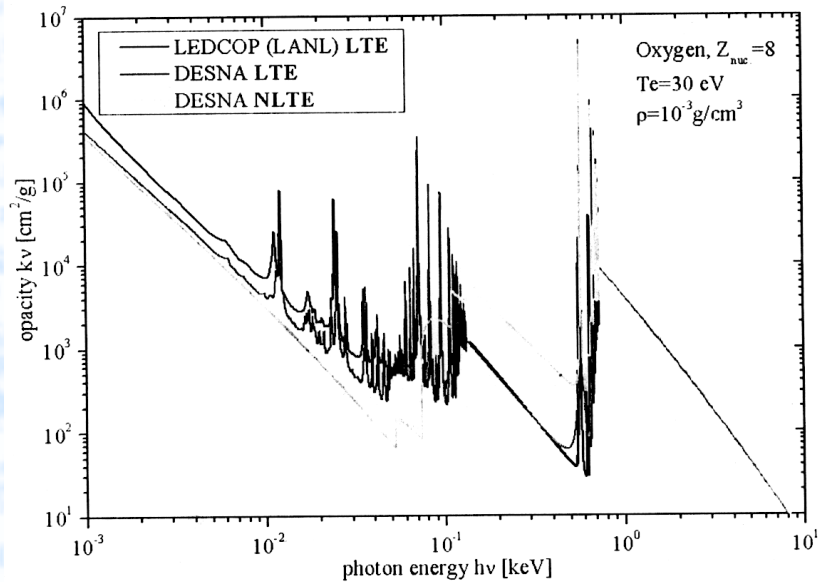
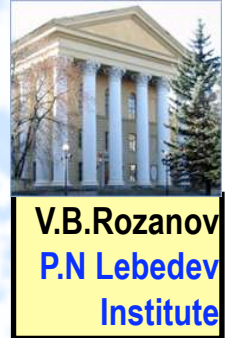


The spectrum of radiation from foam target with 10% addition (on density) of Sn. Simulation for different laser intensity irradiation. Spectral efficiency in 2% BW is 5%. (RFNC-VNIIEF, Sarov, 2006)



The radiation spectrum of Sn target under CO₂ laser irradiation, intensity $\sim 10^{11} \text{ W/cm}^2$ (TRINITI, 2005)

Radiative characteristics of plasma

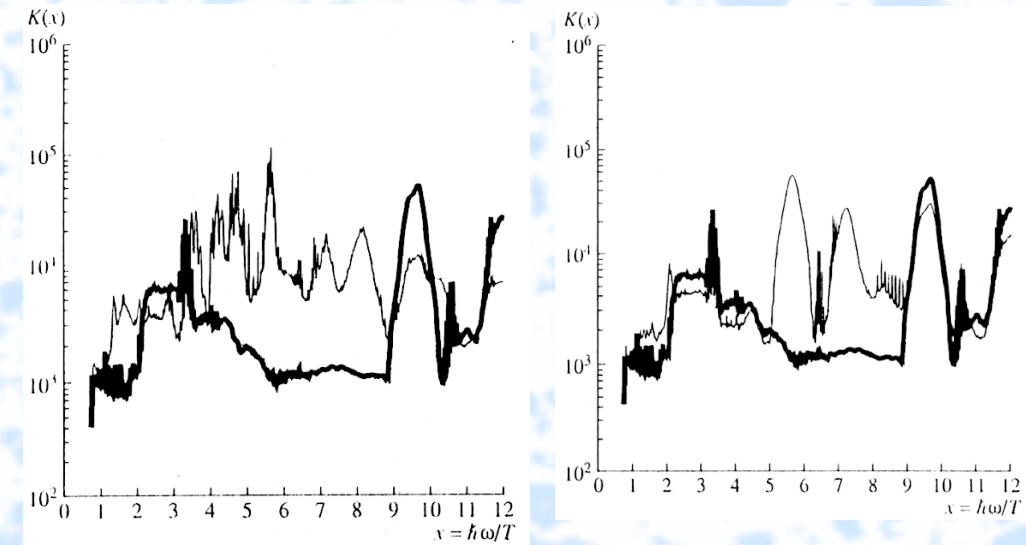


Au:W:Gd:Pr:Ba:Sb

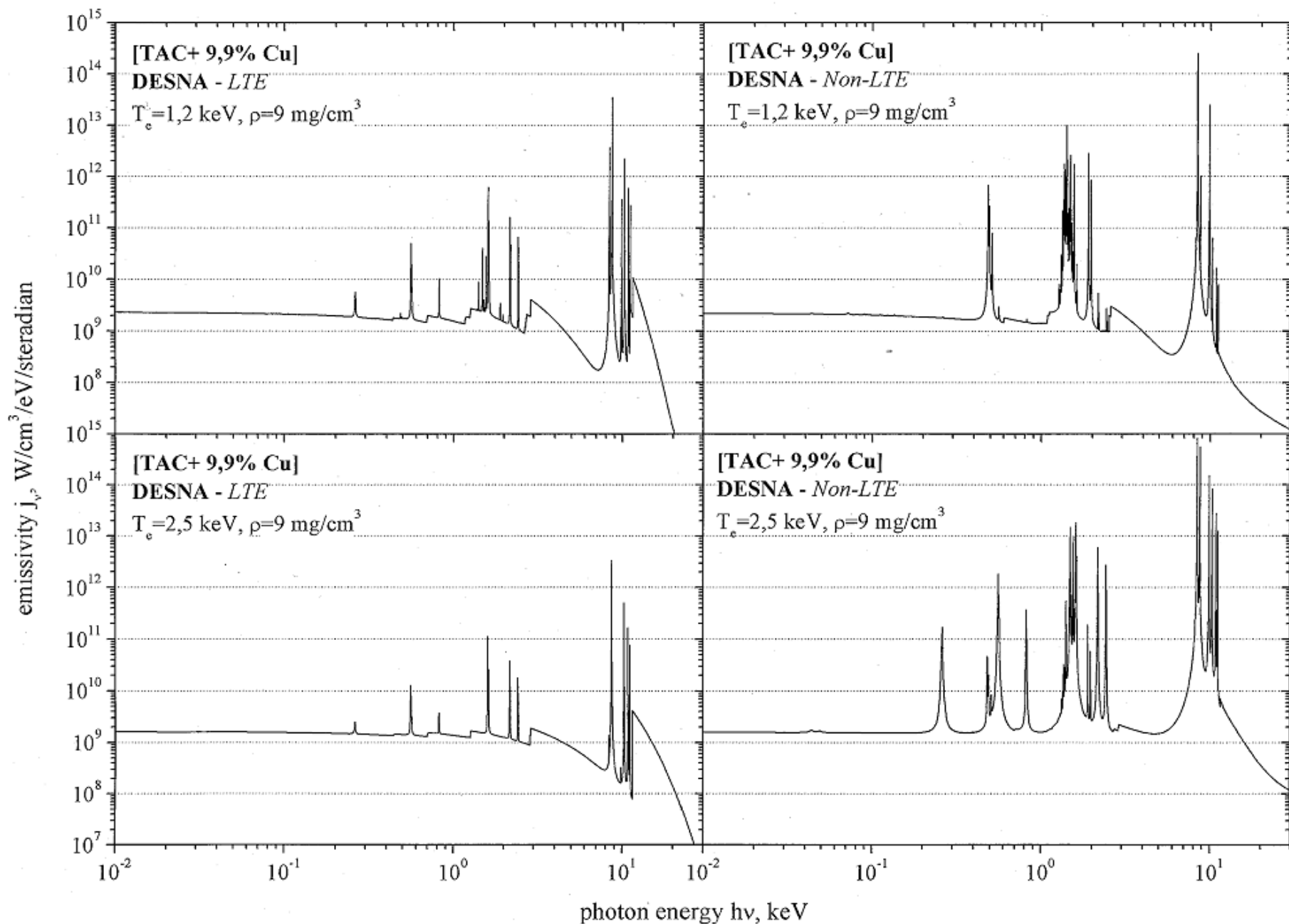
$T=250 \text{ eV}, 1 \text{ g/cm}^3$. (N.Orlov)

for Oxygen radiation near 13-14 nm
(DESNA code - P.N.Lebedev
Institute, 2006)

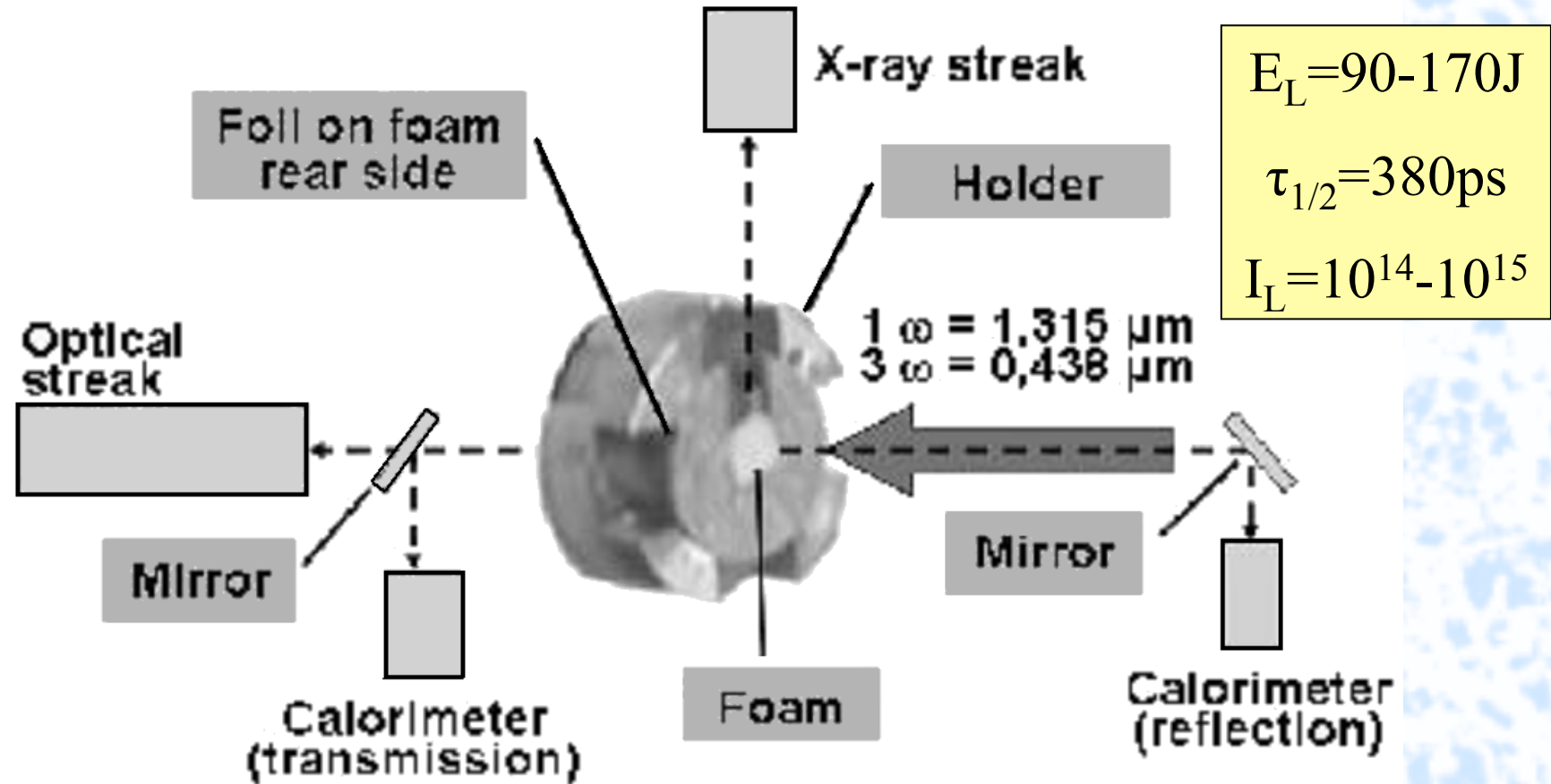
Au:Gd
for radiation in the range
 $h\nu \sim 100 - 500 \text{ eV}$



Plasma spectral emissivity



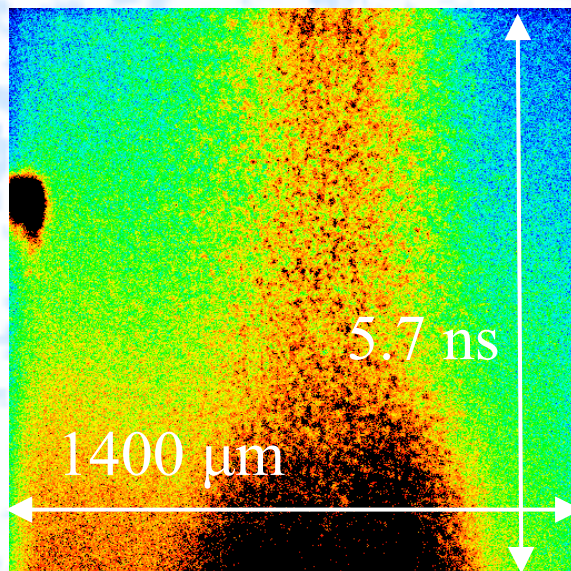
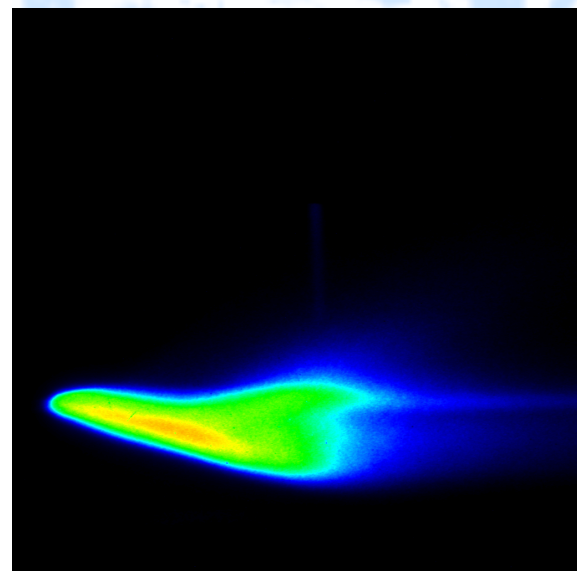
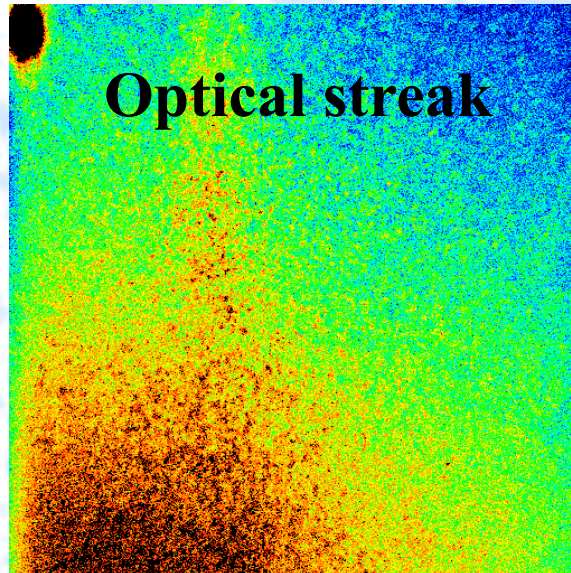
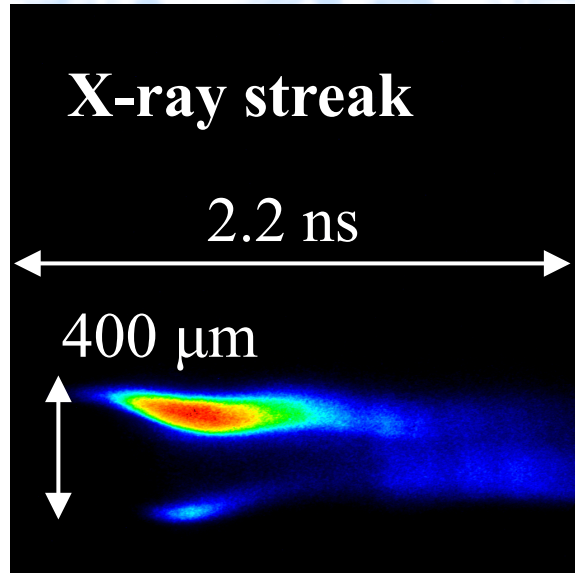
PALS experiment scheme



- Energy transfer in low-density porous targets doped by heavy elements, *V. Rozanov, D. Barishpoltsev, G. Vergunova, S. Gus'kov, N. Demchenko, I.Ya. Doskoch, E. Ivanov, E. Aristova, N. Zmitrenko, J. Limpouch, D. Klir, E. Krousky, K. Masek, V. Kmetik, J. Ullschmied, J. Phys.: Conf. Ser., 112, 022010 (2008)*

PALS experiments (1)

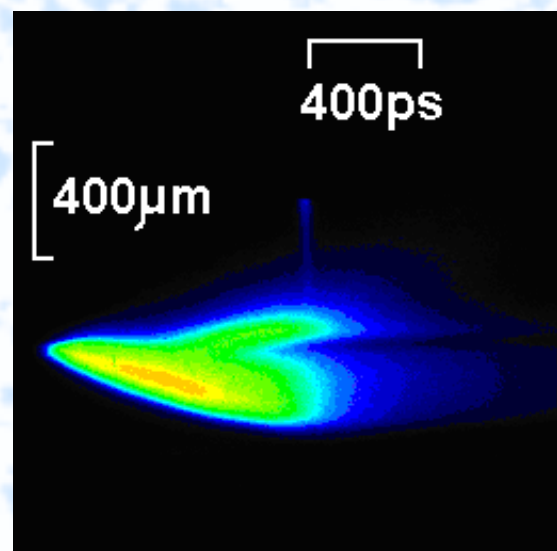
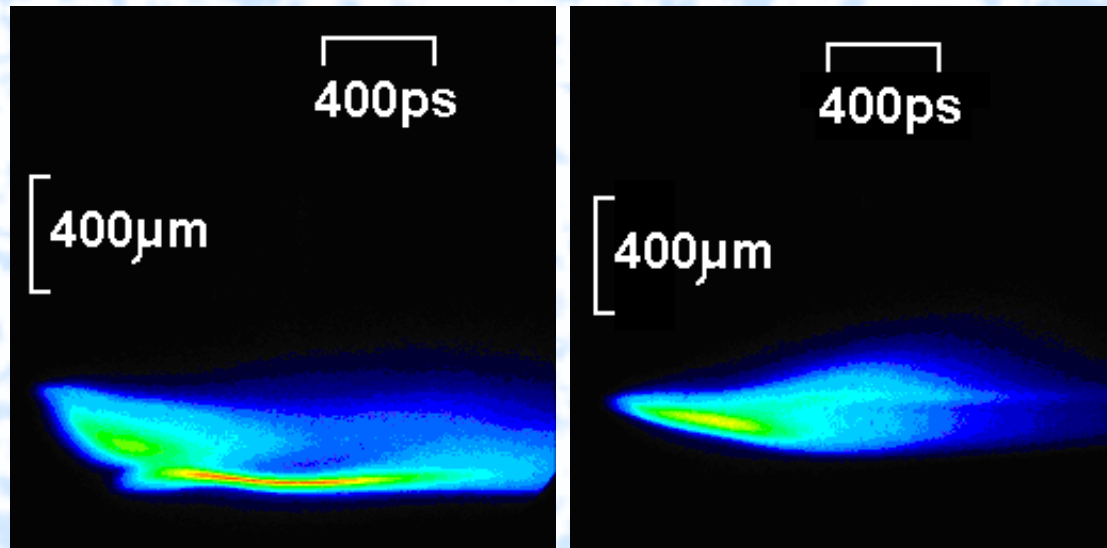
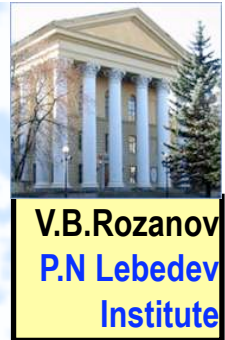
Foam target



Focus: **300 μm in front**
Incid.Energy: **173 J**
Frequency: **$1\omega, 1.315\mu\text{m}$**
Foam type: **TAC**
Density: **9.1 mg/cm³**
Thickness: **400 μm**
Foil: **Al, 5 μm**

Focus: **300 μm in front**
Incid.Energy: **166.4 J**
Frequency: **3ω**
Foam type: **TAC+Cu(9.9%)**
Density: **9.1 mg/cm³**
Thickness: **400 μm**
Foil: **Al, 5 μm**

PALS experiments (2) Foam target



PALS experiments:

$E_L \sim 150 \text{ J}$, $\lambda_3 = 0.454 \mu\text{m}$

$I_L = 3 \cdot 10^{14}$

TAC, $400\mu\text{m} + \text{Al}, 5\mu\text{m}$

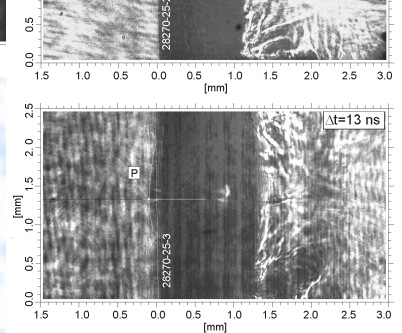
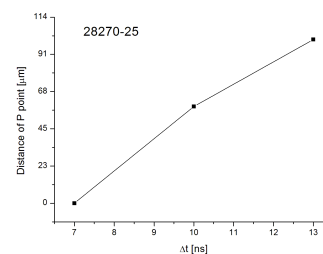
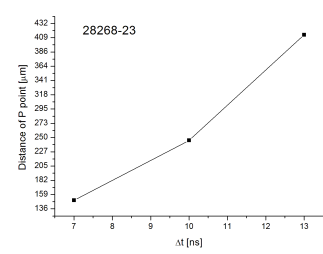
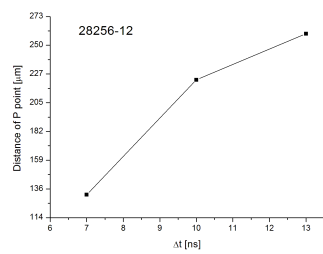
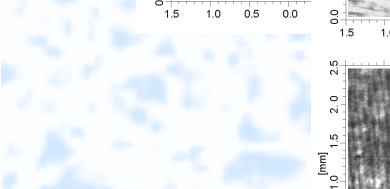
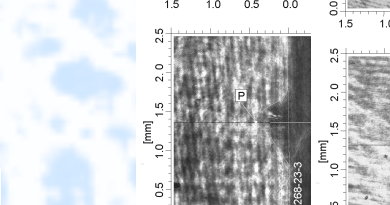
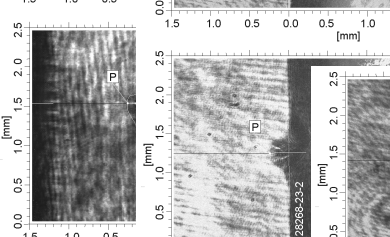
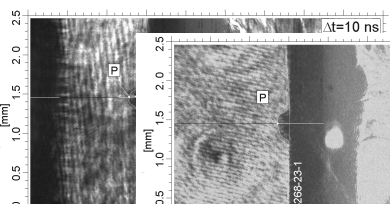
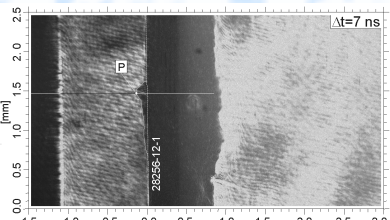
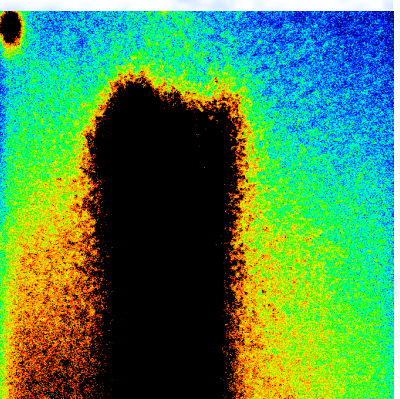
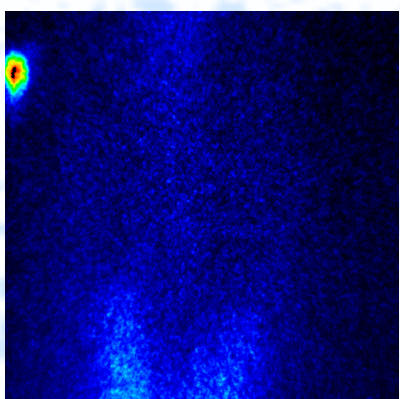
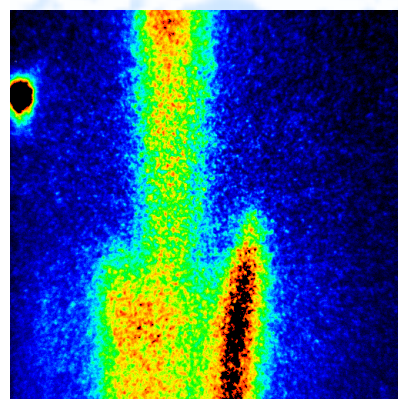
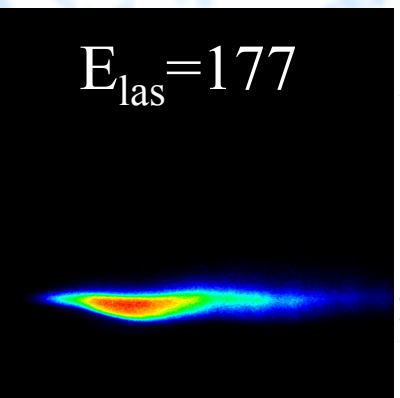
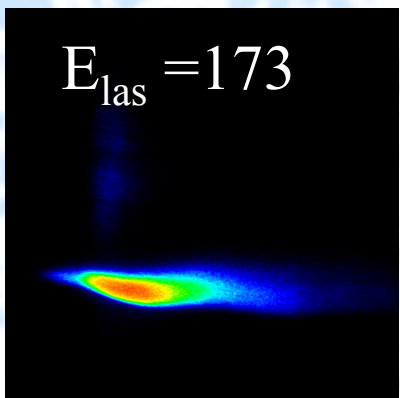
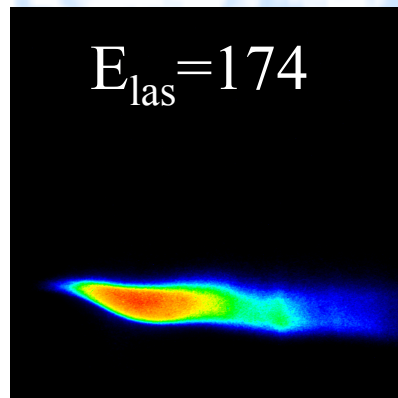
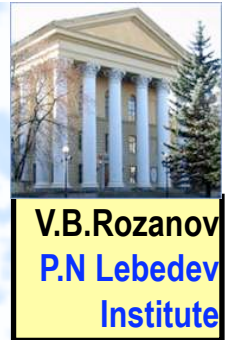
a) $\rho = 4.5 \text{ mg/cm}^3$

b) $\rho = 9.1 \text{ mg/cm}^3$

c) $\rho = 9.1 \text{ mg/cm}^3 + 9.9\% \text{ Cu}$

PALS experiments (3)

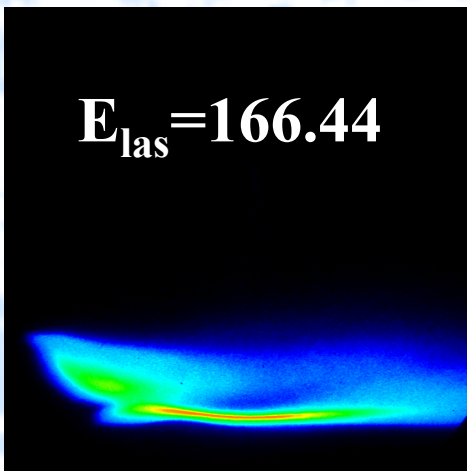
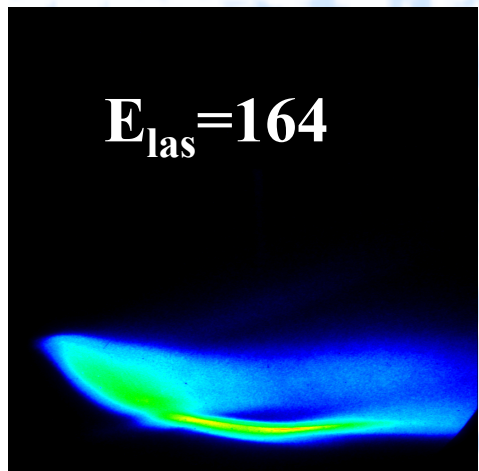
TAC 4.5 mg/cm³, 1 ω



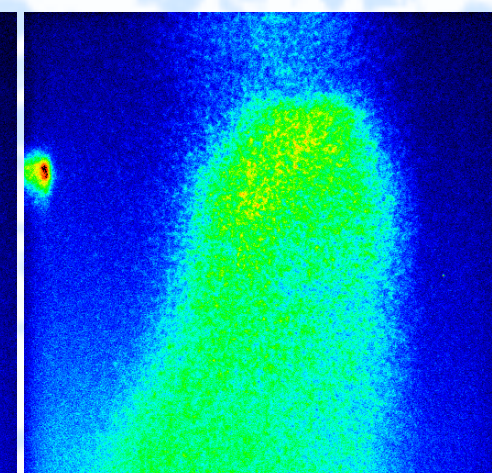
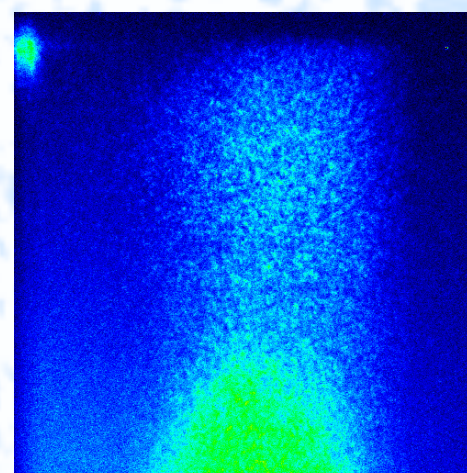
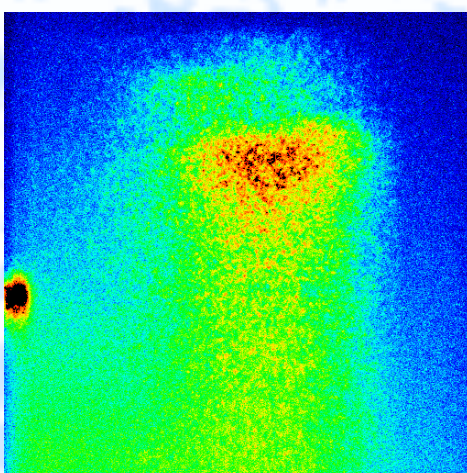
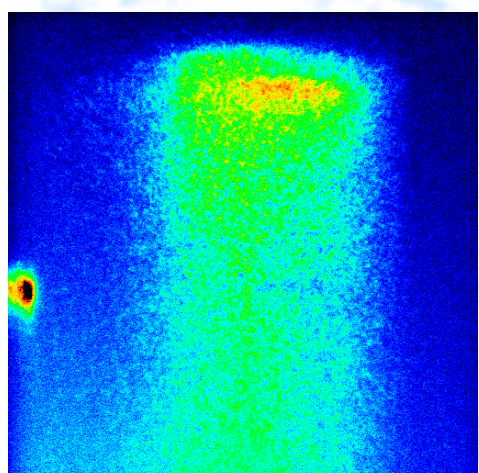
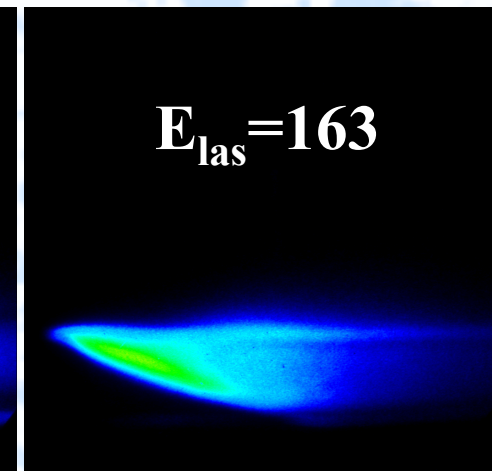
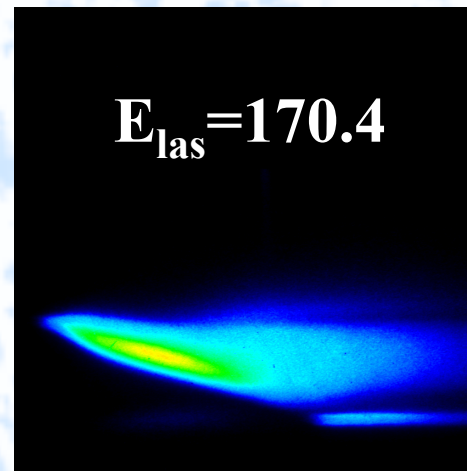
PALS experiments (4)



TAC 4.5 mg/cm³, 3ω

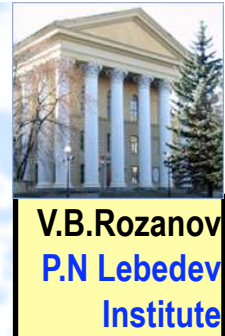
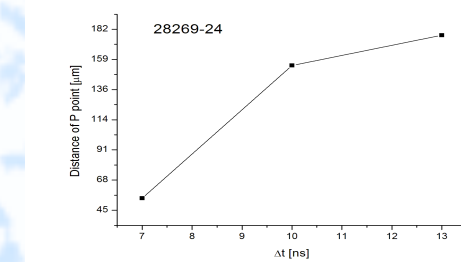
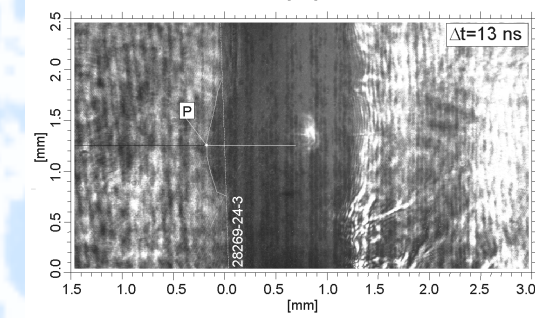
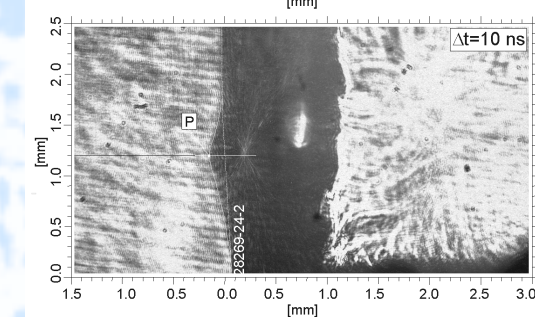
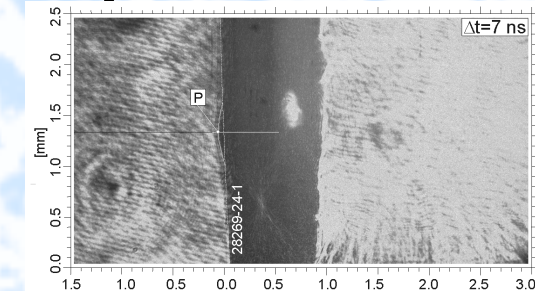
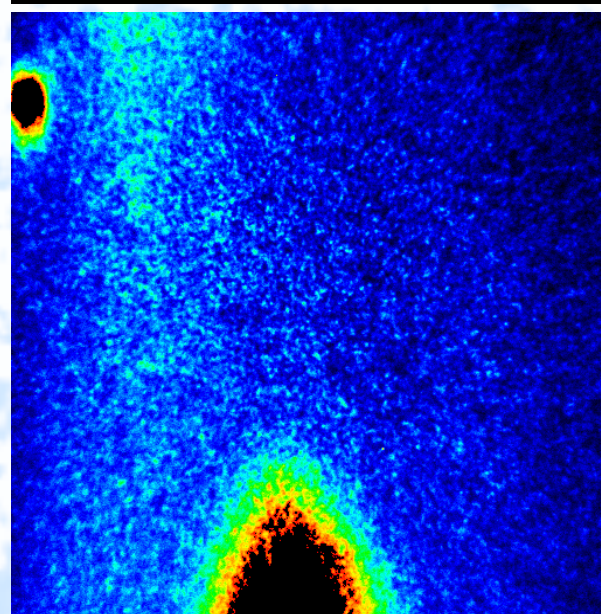
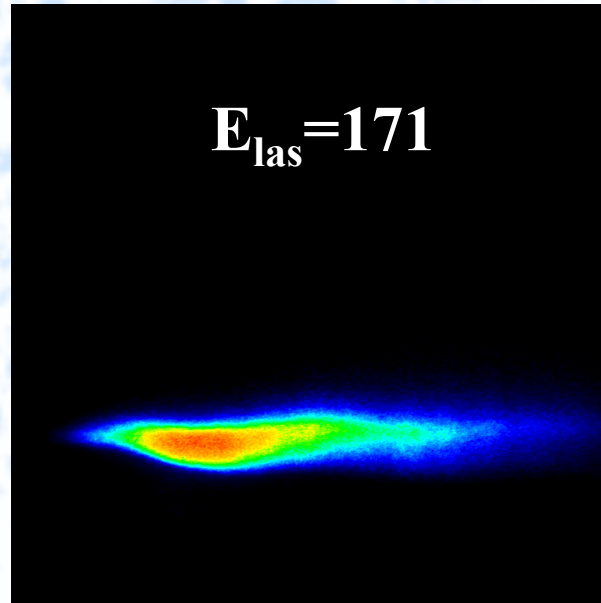


TAC 9.1 mg/cm³, 3ω

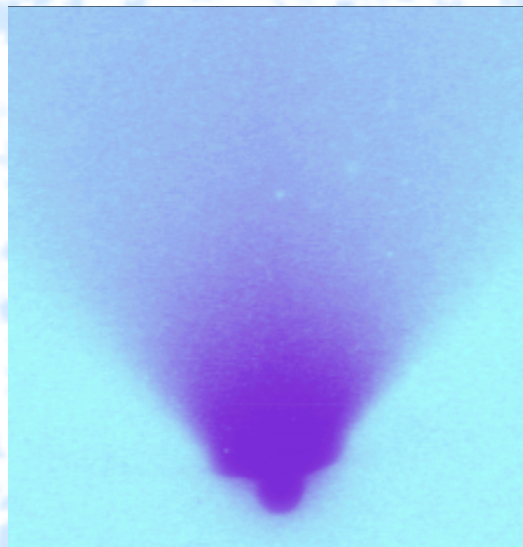
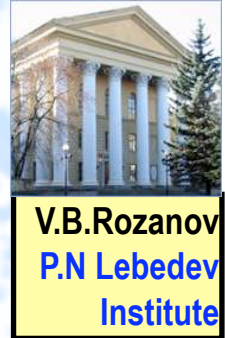


PALS experiments (5)

TAC+Cu 9.1 mg/cm³, 1 ω



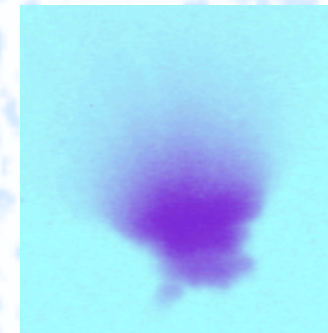
Experiment (TRINITI, 2004)



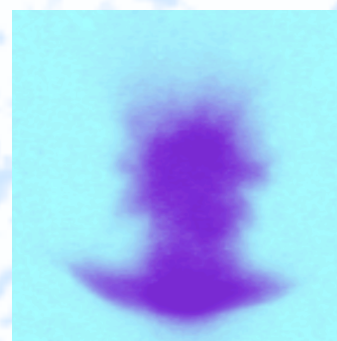
Ni foil, $d=0.6 \mu\text{m}$

Laser beam

Target



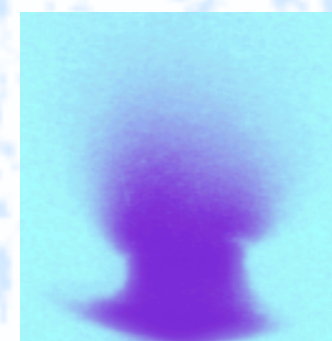
Agar, $d=300 \mu\text{m}$,
 $\rho=2 \text{ mg/cm}^3$



500 μm



Ni



Agar ($d=300 \mu\text{m}$, $\rho=2 \text{ mg/cm}^3$) with
Ni foil ($d=0.6 \mu\text{m}$) at the rear surface

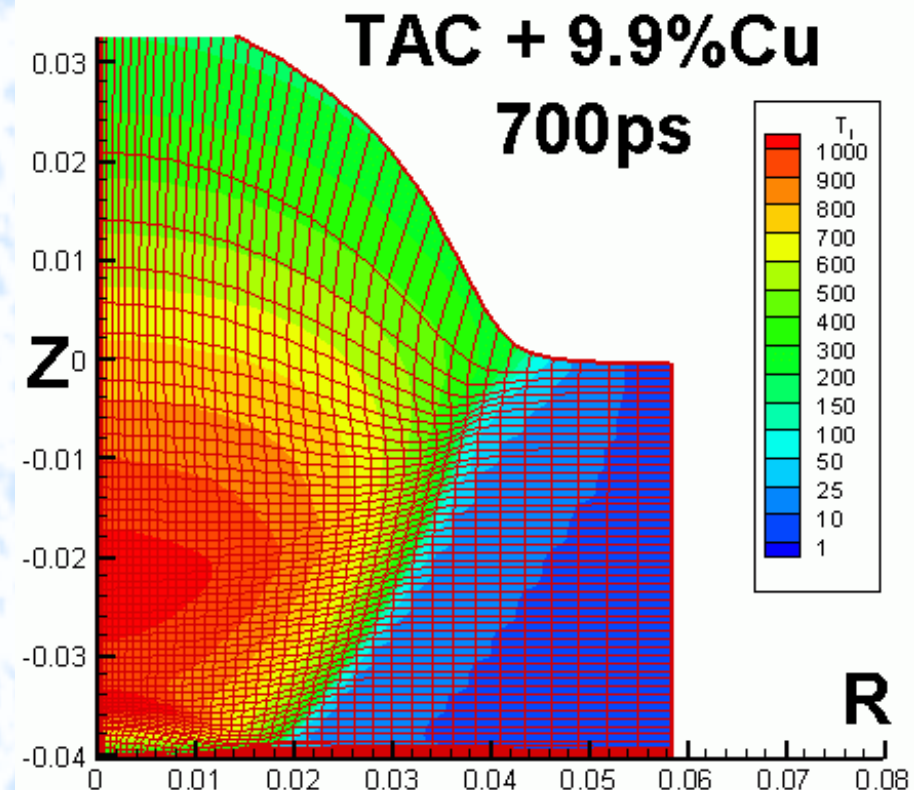
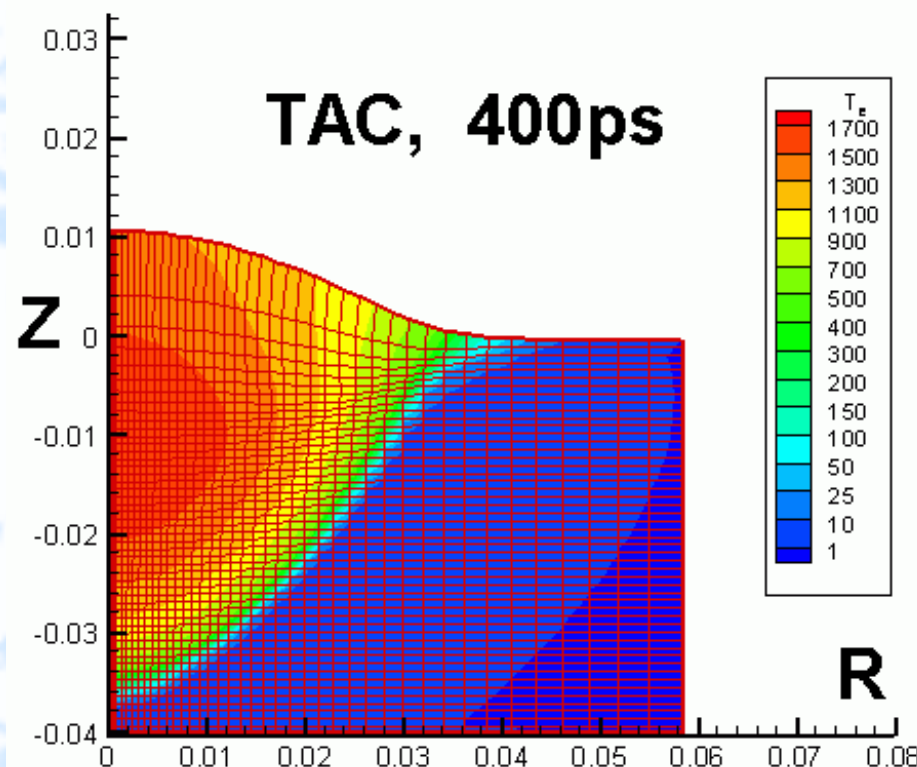
Agar ($d=300 \mu\text{m}$, $\rho=1 \text{ mg/cm}^3$) doped by
 CuCl_2 ($\rho=1 \text{ mg/cm}^3$) with Ni foil ($d=0.6 \mu\text{m}$)
at the rear surface



Simulation: LATRANT 2D

Homogeneous media radiation transport

(LPI, IMM, 2006)

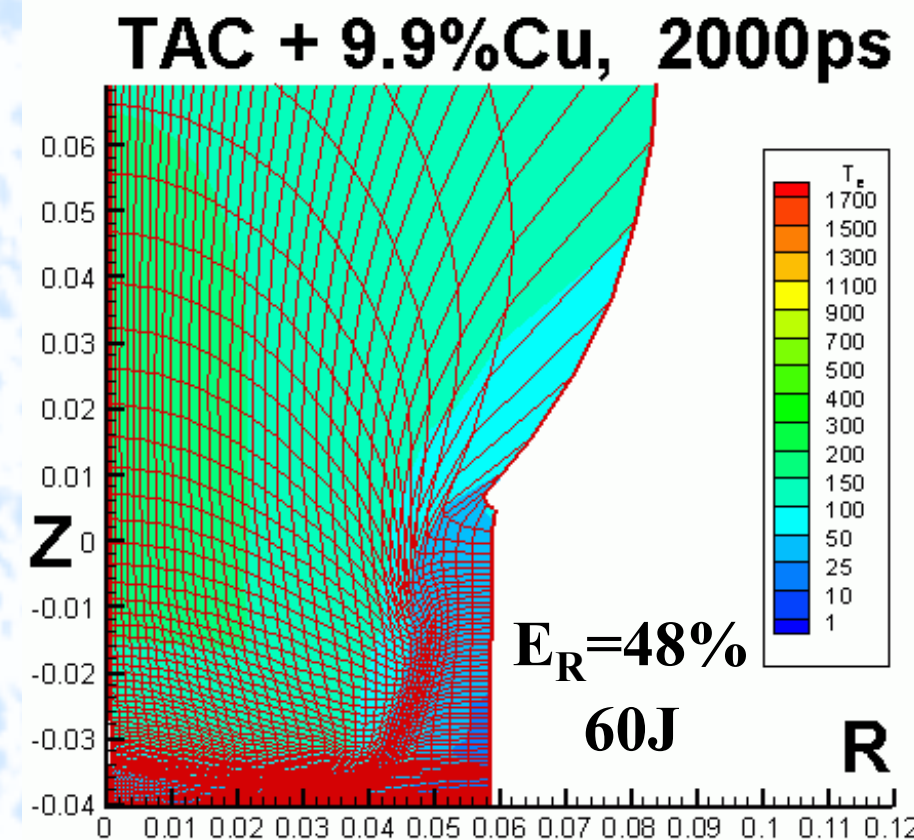
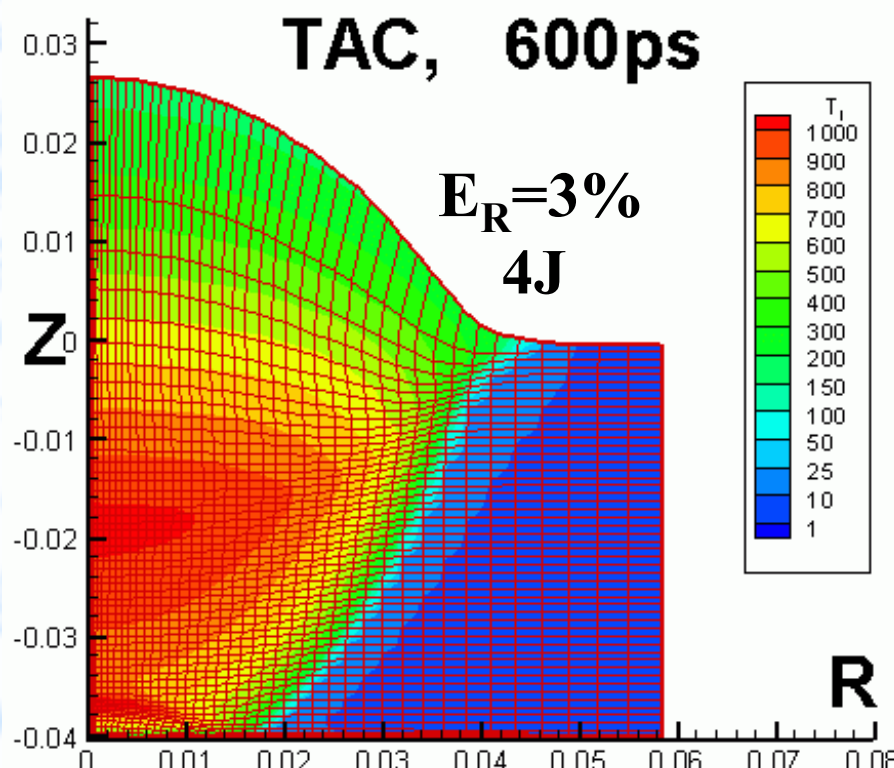




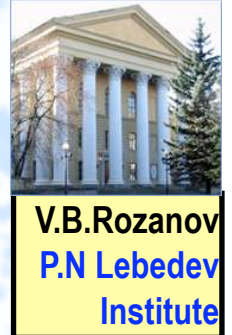
Simulation: LATRANT 2D

Homogeneous media radiation transport

(LPI, IMM, 2006)



Theoretical model for PALS experiment (1)



Includes:

- Strong point explosion model:
$$R = \left[\frac{75}{16\pi} \frac{(\gamma - 1)(\gamma + 1)^2}{(3\gamma - 1)} \right]^{1/5} \left(\frac{Et^2}{\rho} \right)^{1/5}$$
- After the end of the laser pulse the plasma behaves like a homogeneous medium, and its further evolution corresponds to the strong point explosion model. The Al foil optical emission allows one to estimate the plasma energy, which turns to be essentially smaller than the laser pulse energy
- Heat wave velocity (x-ray streak) depends on electron heat conductivity (we can choose the flux limiter value)
- Laser energy reflection strongly depends on electron heat conductivity rate: low rate heat conductivity → high reflection level

Theoretical model for PALS experiment (2)



- Effective equation of state of the foam (relaxation):
- The life time of dense structures is limited by the ion viscosity
- EOS for Al:

ρ/ρ_0	p (Mbar)	$T, {}^0\text{K}$	$D, \text{km/s}$	$U, \text{km/s}$
1.39	0.56	1300	8.6	2.4
1.55	0.99	3000	10.2	3.6
1.7	1.53	5600	11.8	4.8



PALS RAPID simulation (1)

$$E_{\text{las}} \sim 100 \text{ J},$$

$$\lambda = 1.315 \mu\text{m}$$

$$\tau_{\text{las}} = 0.38 \text{ ns at } 1/2q_{\text{max}} \text{ for } 1\omega;$$

$$\tau_{\text{las}} = 0.32 \text{ ns at } 1/2q_{\text{max}} \text{ for } 3\omega$$

$$q_{\text{las}} = 3.6 \cdot 10^{14} \text{ W/cm}^2$$

Target: TAC-foam (380 μm) + Al (5 μm)

Foam density: 4.5 mg/cm³ and 9.1 mg/cm³

Simulation:

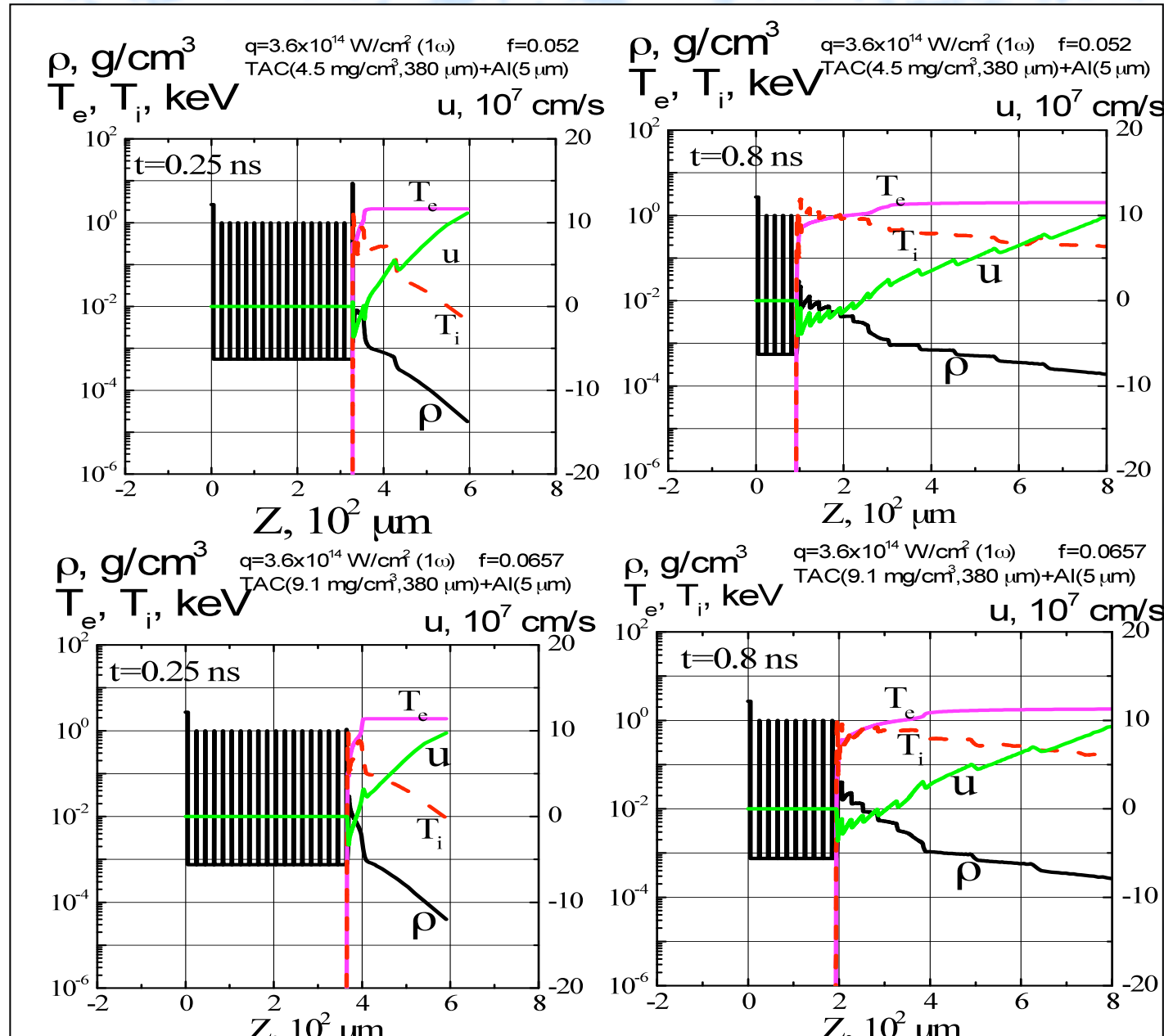
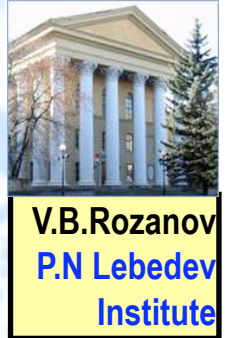
Hydrodynamic code RAPID, 20 thin solid layers separated by low-density gas.

Average density equals to foam density. Flux-limited electron thermal conductivity:

$$W_e = \frac{W_{Sp} W_{max}}{W_{Sp} + W_{max}}, \text{ where } W_{Sp} \quad \text{-- Spitzer flux,}$$

$$W_{max} = f n_e T_e (T_e / m_e)^{1/2} \quad \text{-- limiting flux, } f \text{ -- flux limiter.}$$

PALS RAPID simulation (2)



$f = 0.052$

$f = 0.0657$

PALS RAPID simulation⁽³⁾



	4.5 mg/cm ³	9.1 mg/cm ³
1 ω	$v_f = 3.25 \cdot 10^7 \text{ cm/s}$ $q = 3.6 \cdot 10^{14}, f = 0.052, d_a = 0.136$ $q = 1.8 \cdot 10^{14}, f = 0.0675, d_a = 0.233$	$v_f = 2.5 \cdot 10^7 \text{ cm/s}$ $q = 3.6 \cdot 10^{14}, f = 0.0657, d_a = 0.159$ $q = 1.8 \cdot 10^{14}, f = 0.0864, d_a = 0.274$
3 ω	$v_f = 8.7 \cdot 10^7 \text{ cm/s}$ $q = 3.6 \cdot 10^{14}, f = 0.0403, d_a = 0.606$ $q = 1.8 \cdot 10^{14}, f = 0.0616, d_a = 0.815$	$v_f = 5.04 \cdot 10^7 \text{ cm/s}$ $q = 3.6 \cdot 10^{14}, f = 0.027, d_a = 0.686$ $q = 1.8 \cdot 10^{14}, f = 0.09, d_a = 0.920$

v_f – average velocity of thermal wave front (experimental value). Table shows the flux limiter values f which provide in simulations the experimental values of velocity v_f . δ_a – simulated value of absorption efficiency (collisional absorption).

1D Hydrodynamic code RAPID include Maxwell equations for heating radiation, the hydrodynamical equations with electron thermal conductivity, the model of the absorption takes into account inverse bremsstrahlung, and anomalous and resonance absorption.

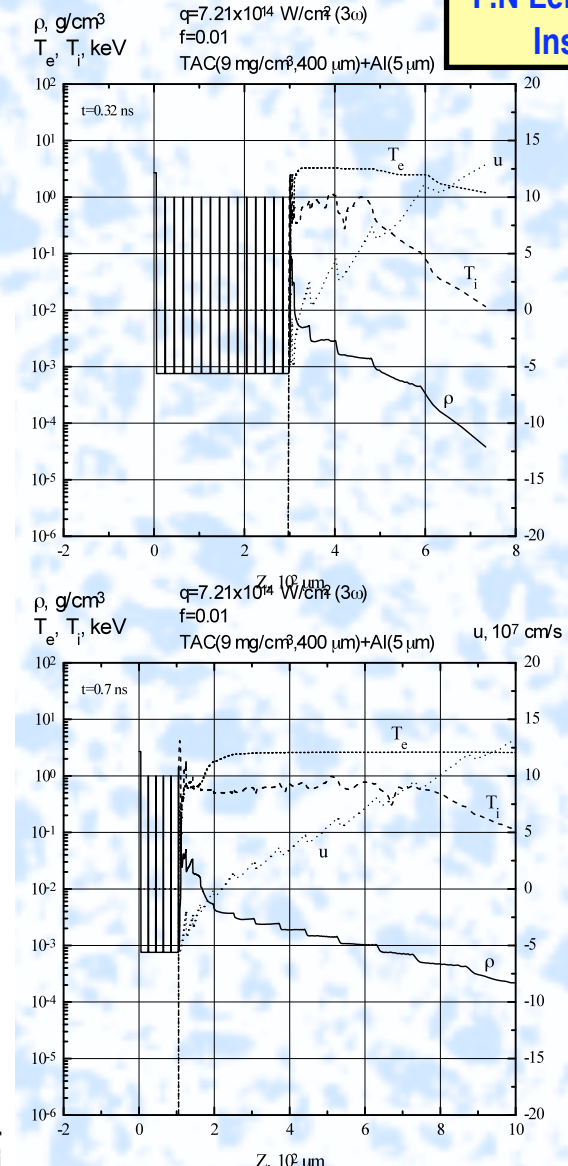
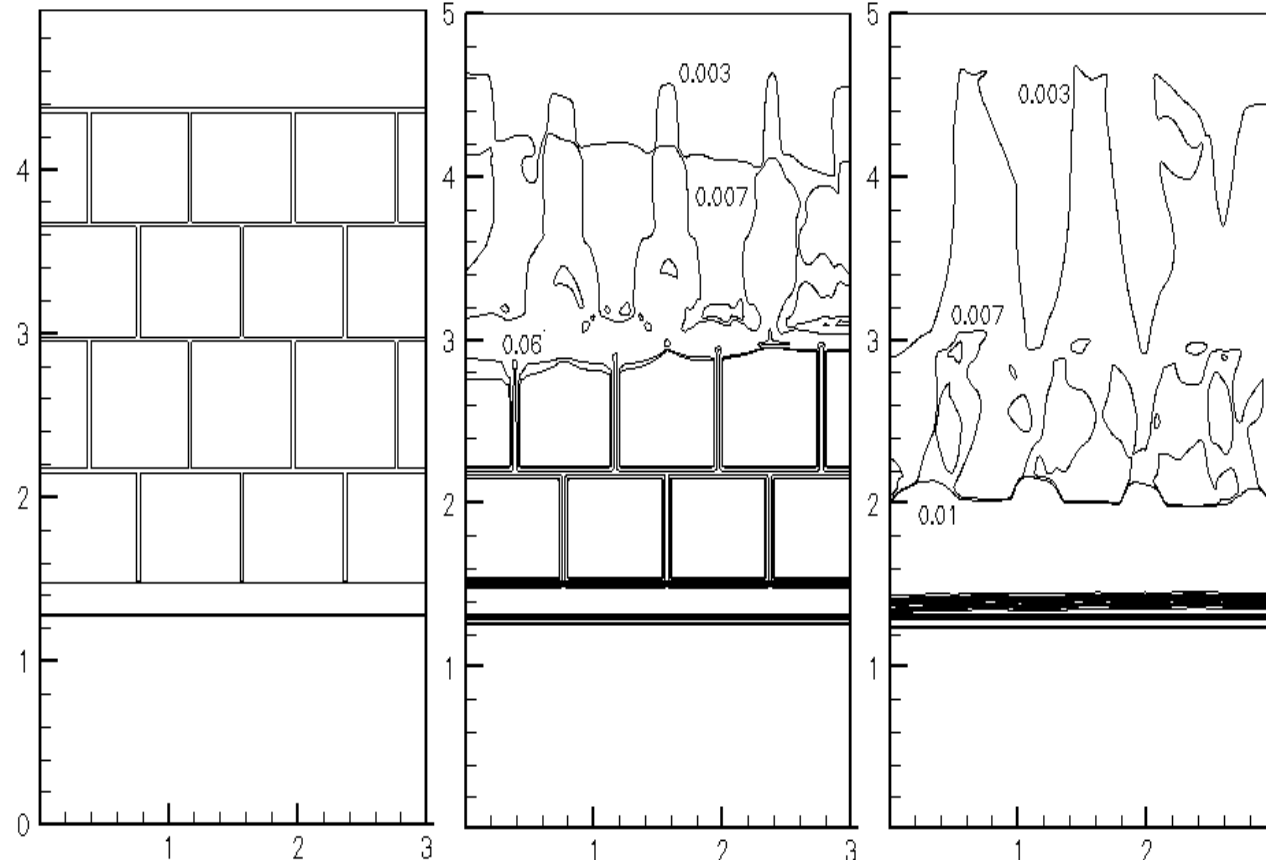
- Yu.A.Afanas'ev, E.G.Gamalii, N.N.Demchenko, O.N.Krokhin, and V.B.Rozanov. Teoretical study of the hydrodynamics of spherical targets taking the refraction of the laser radiation into account, *Zh.Eksp. Teor.Fiz.* **79**, 837-849, 1980. *Sov. Phys.JETP* **52** (3), 1980
- S.Yu.Gus'kov, N.N.Demchenko, V.B.Rozanov, R.V.Stepanov, N.V.Zmitrenko, A.Caruso, C.Strangio. Symmetric compression of 'laser greenhouse' targets by a few laser beams, *Quantum Electronics*, **33**(2003)

PALS RAPID simulation⁽⁴⁾



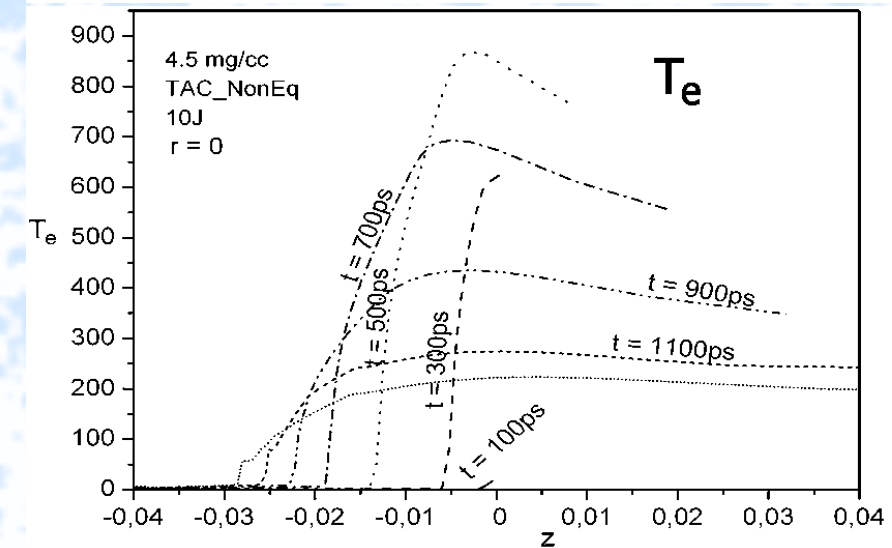
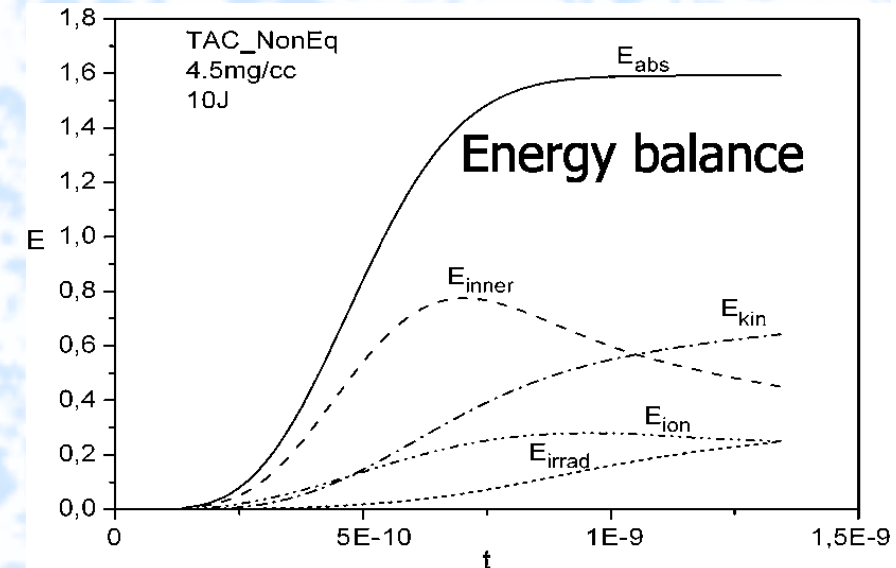
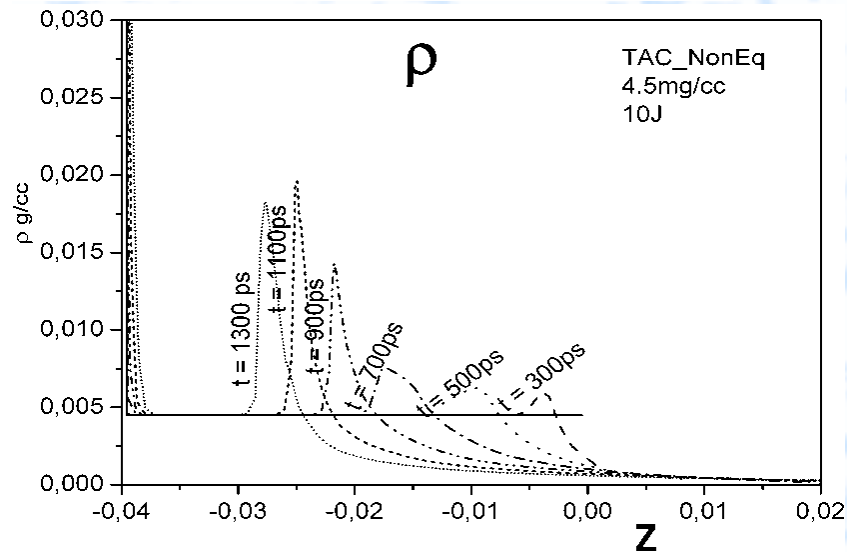
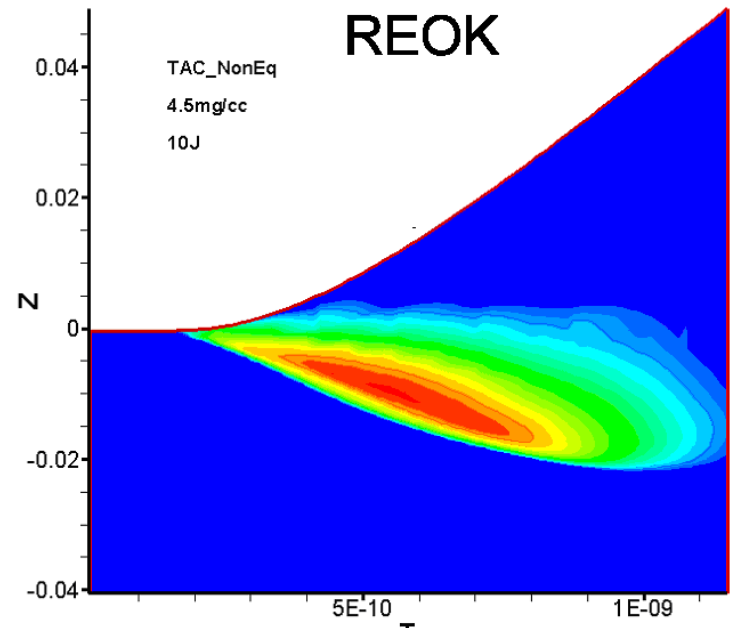
V.B.Rozanov
P.N Lebedev
Institute

NUTCY 2D, RAPID 1D codes:
laser-irradiated structured media
(LPI, IMM, 2006)



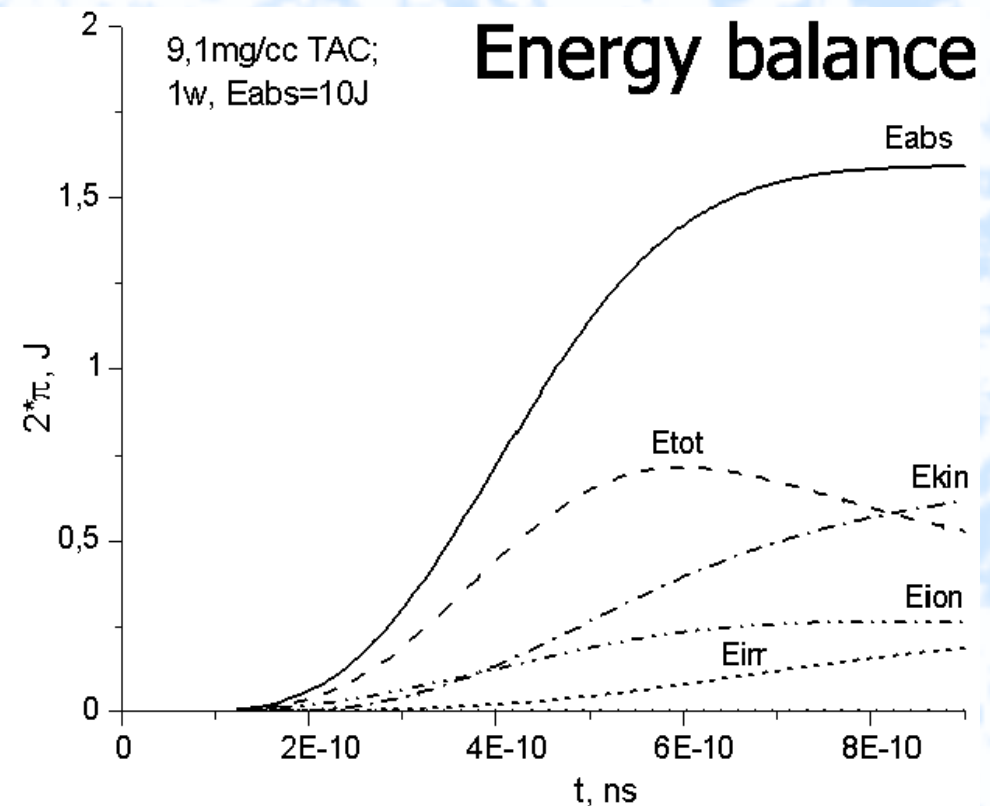
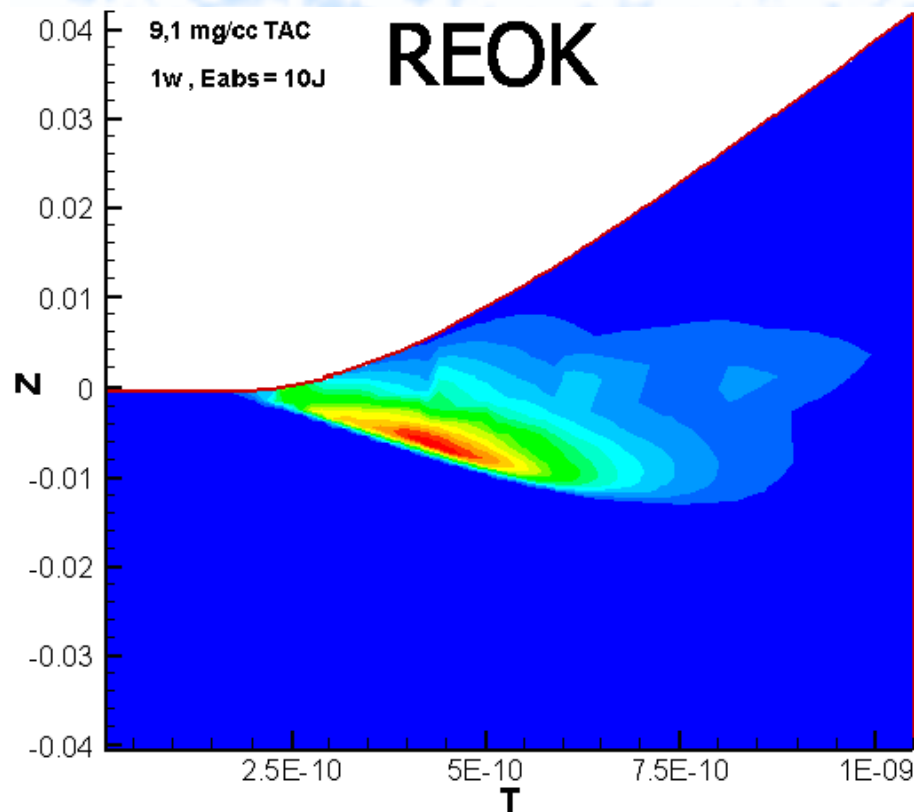
PALS Numerical simulations⁽⁵⁾

TAC 4.5 mg/cm³, 1 ω , 10J, r=0



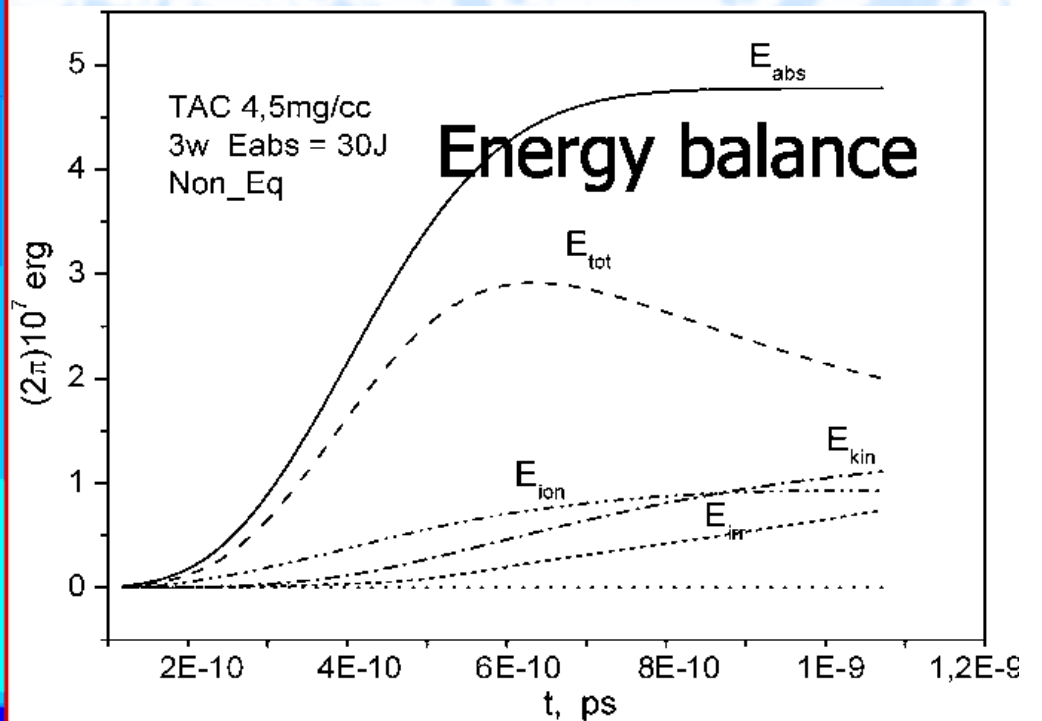
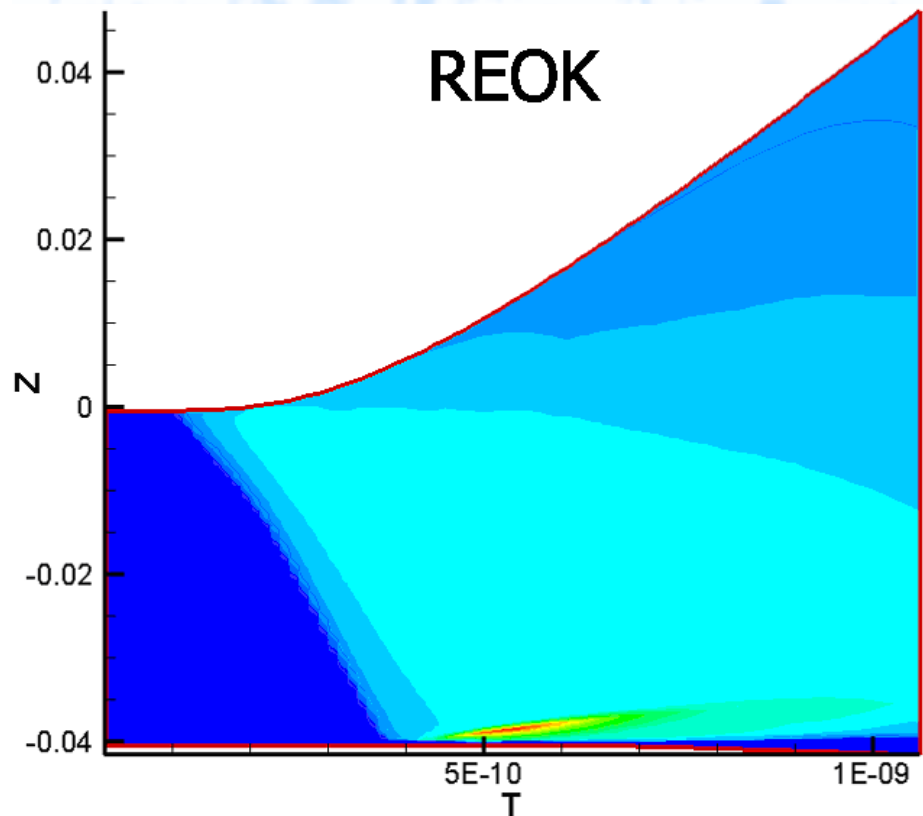
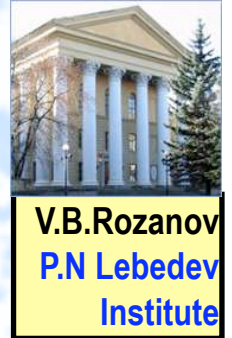
PALS Numerical simulations⁽⁶⁾

TAC 9.1 mg/cm³, 1 ω , 10J



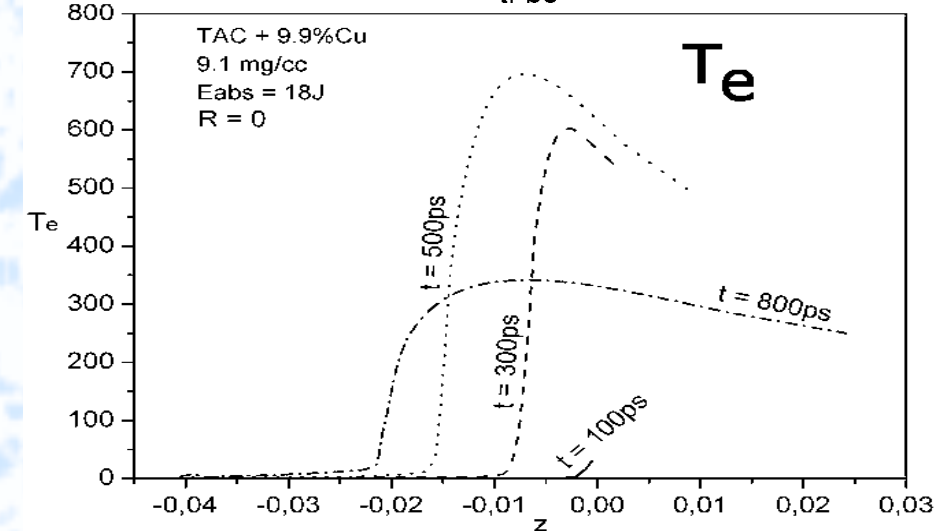
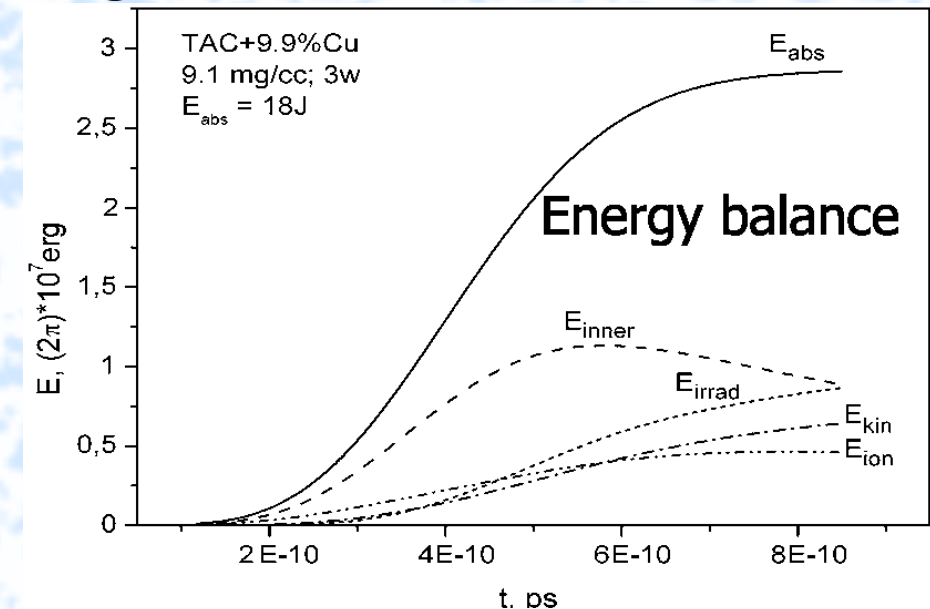
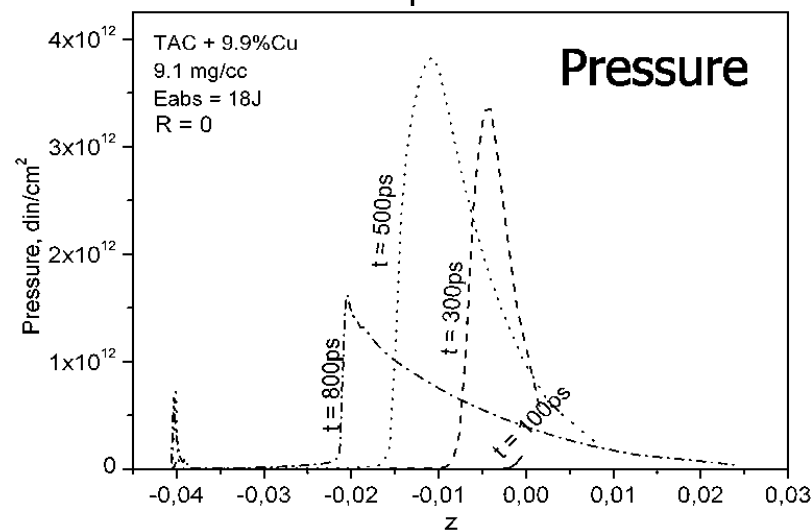
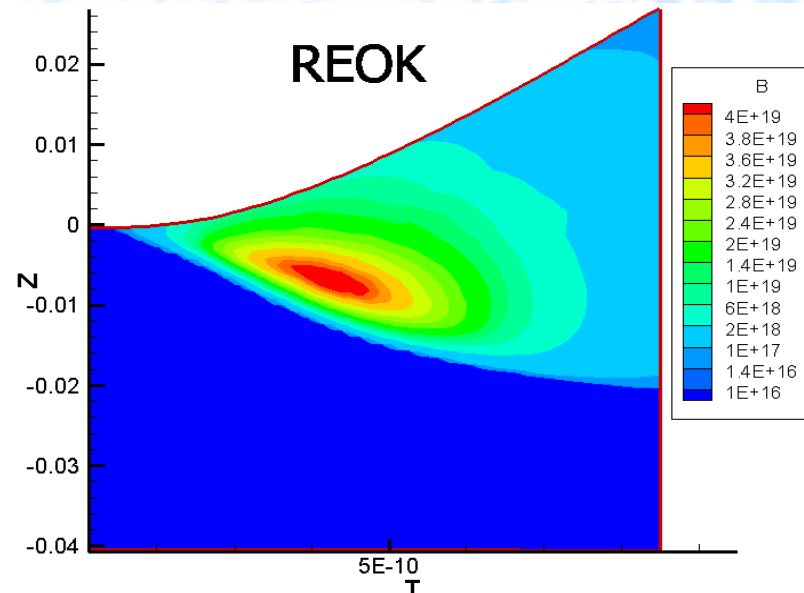
PALS Numerical simulations⁽⁷⁾

TAC 4.5 mg/cm³, 3ω, 30J



PALS Numerical simulations(8)

TAC +Cu 9.9% = 9.1 mg/cm³, 3ω, 18J, r=0

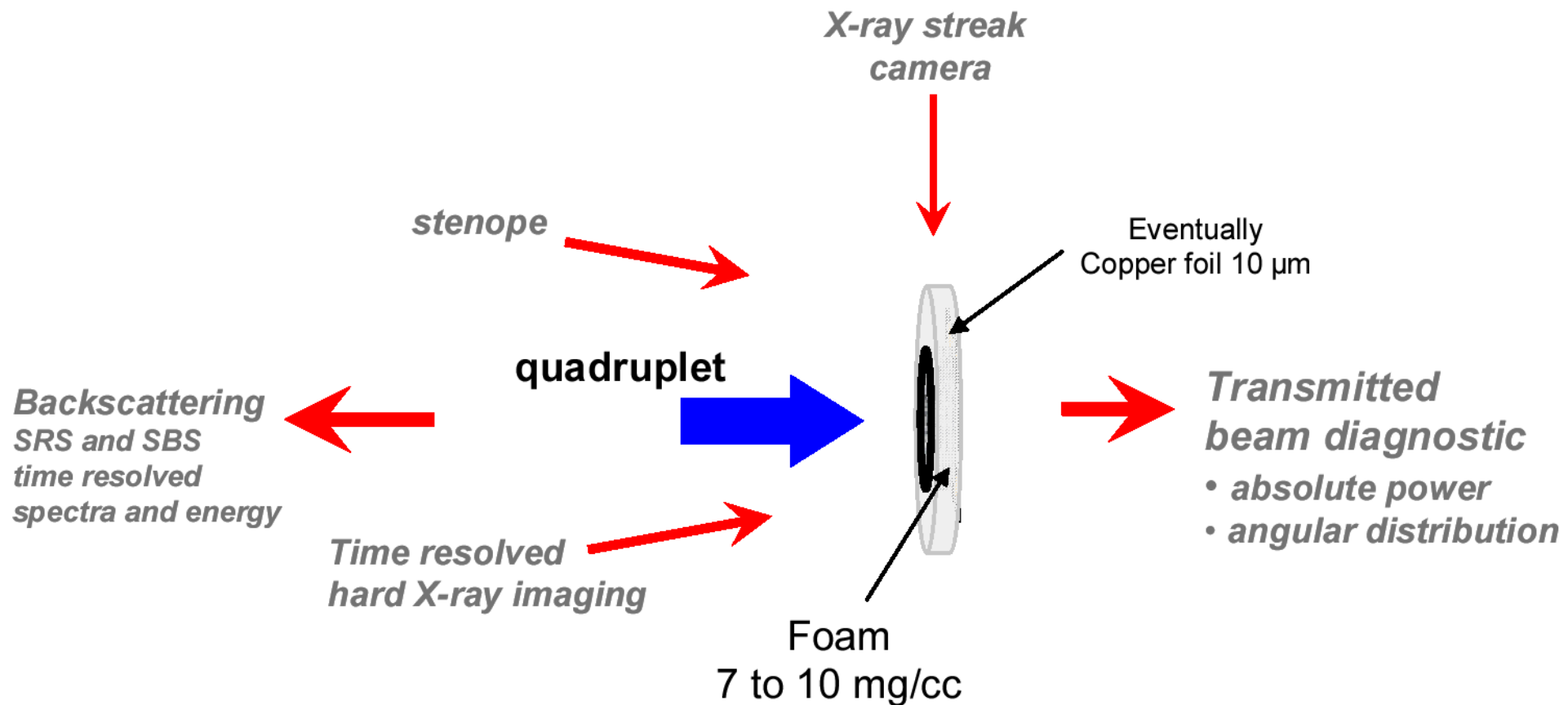


LIL experiments (1)

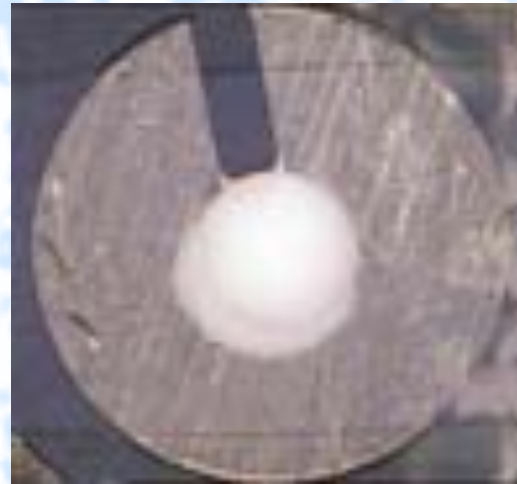
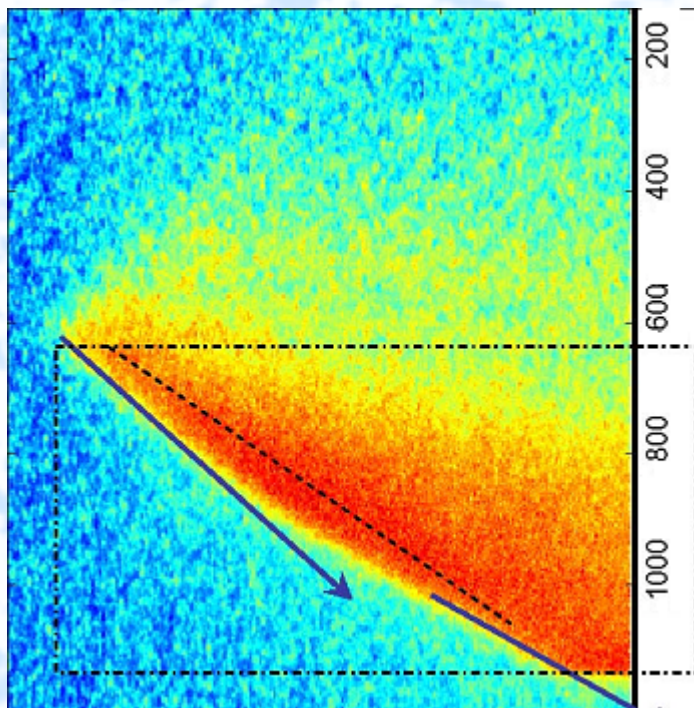


$E_{\text{las}} \sim 10 \text{ kJ}$,
 $\tau_{\text{las}} = 2.5 \text{ ns}$ at $1/2 q_{\max}$
Target: TMPTA-foam (900 μm)
Foam density: 6.5 - 10 mg/cm³

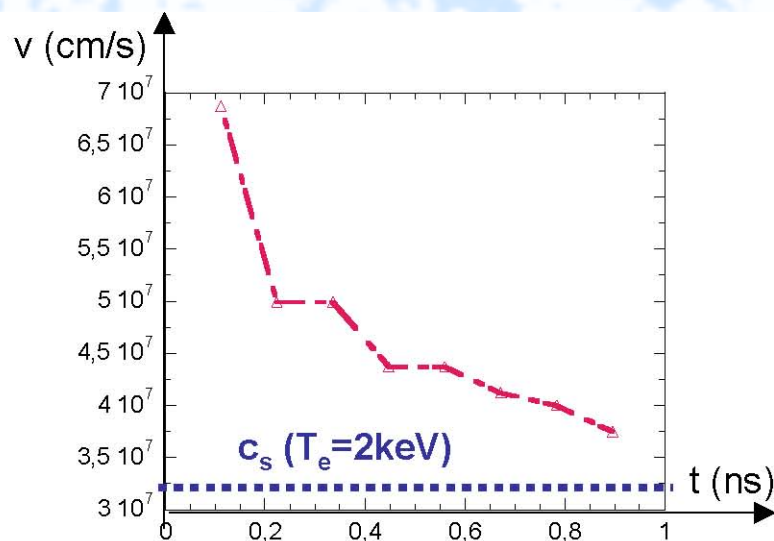
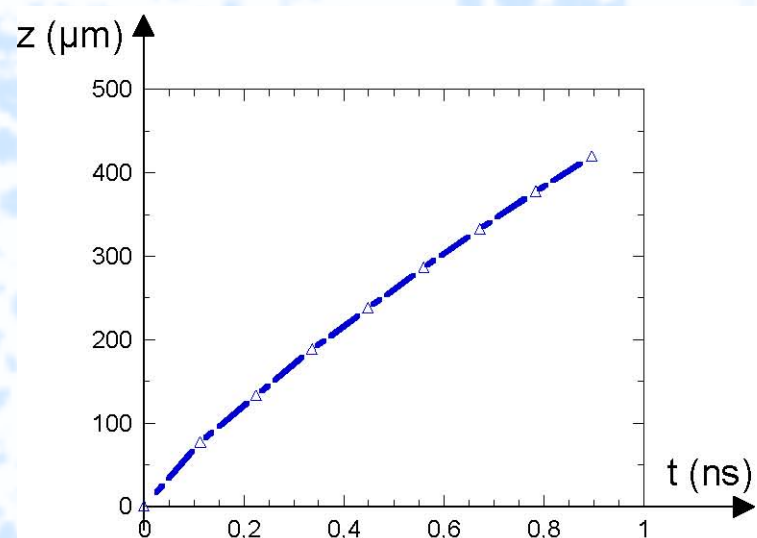
$$\lambda = 0.351 \text{ } \mu\text{m}$$
$$q_{\text{las}} = 4 \cdot 10^{14} \text{ W/cm}^2$$



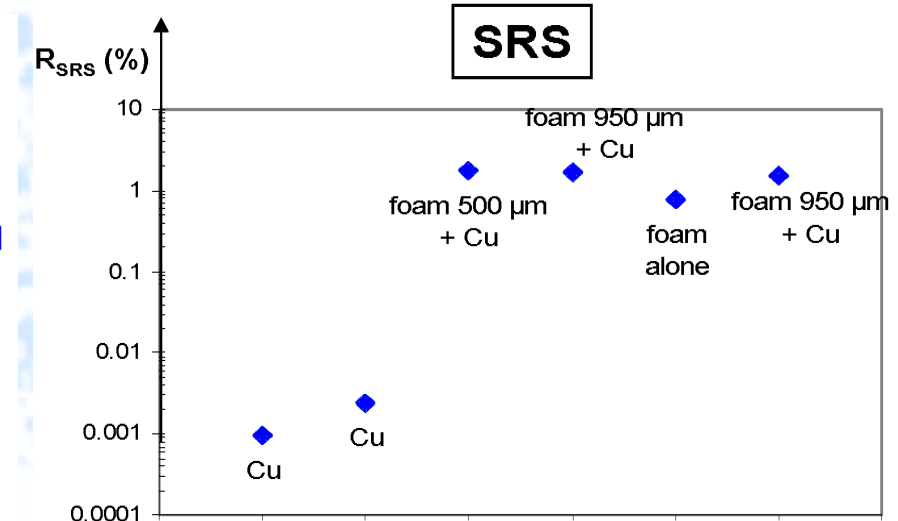
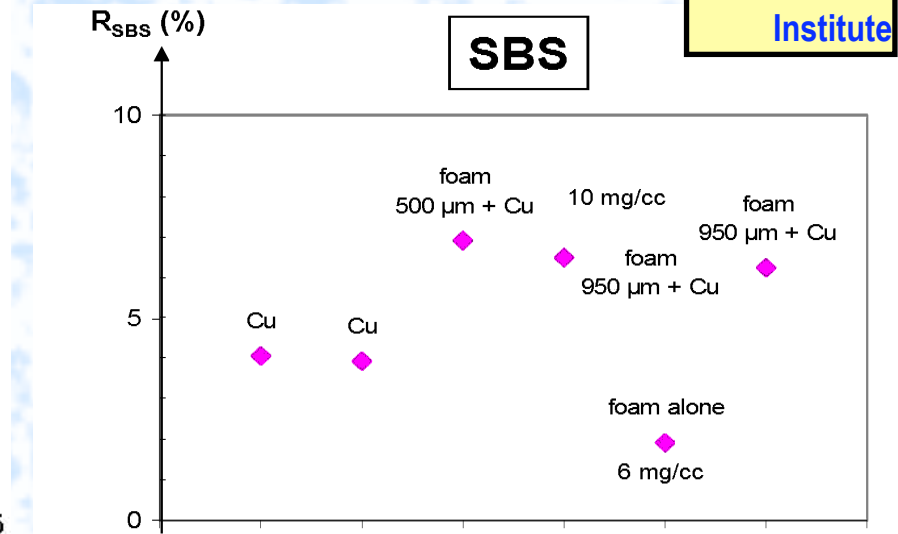
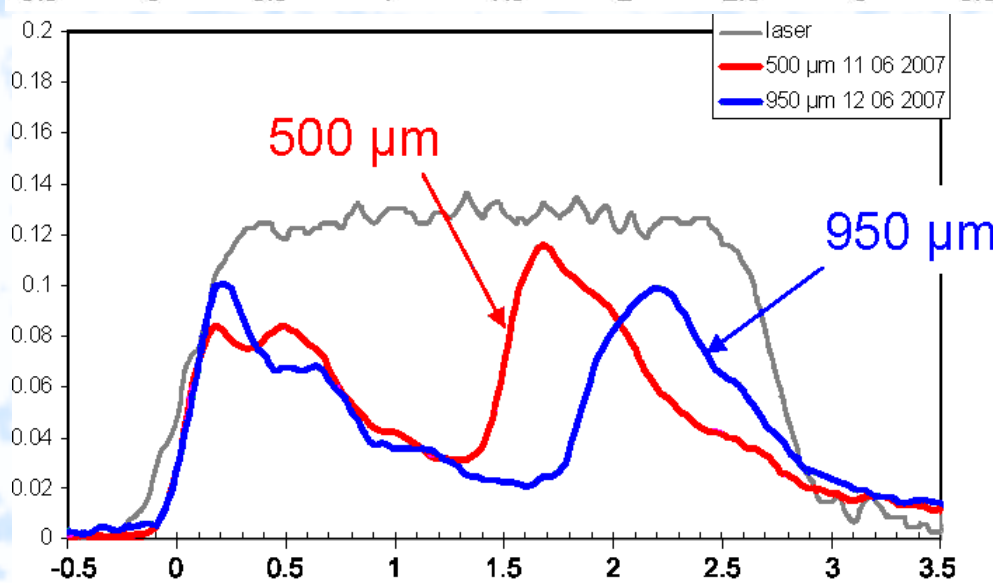
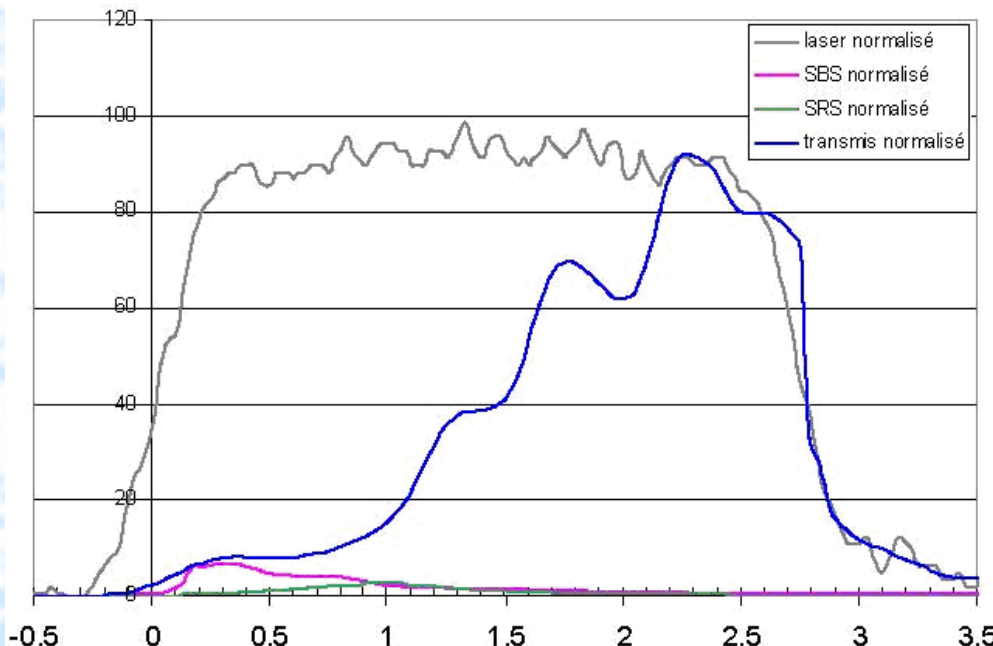
LIL experiments (2)



LIL target photo

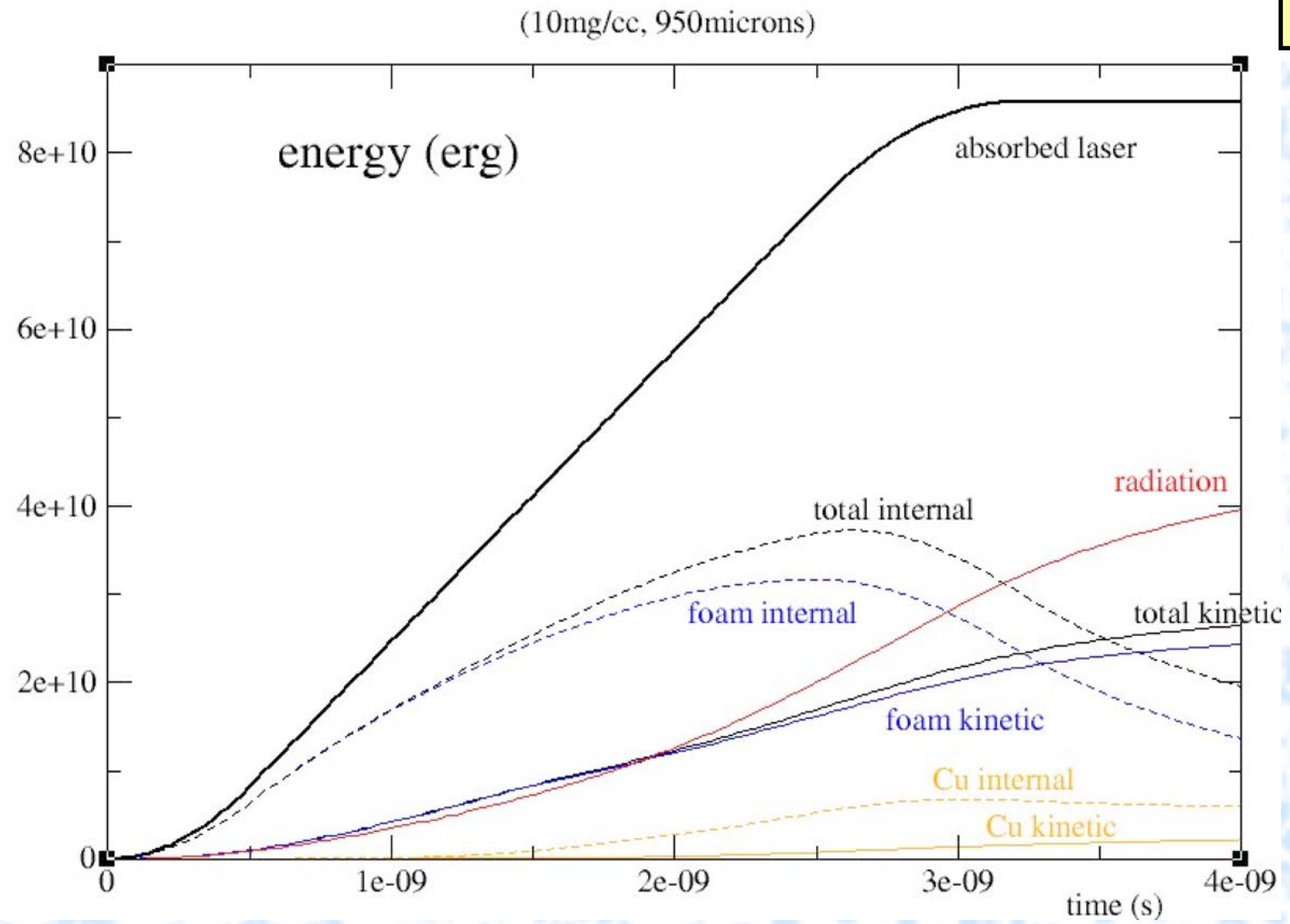
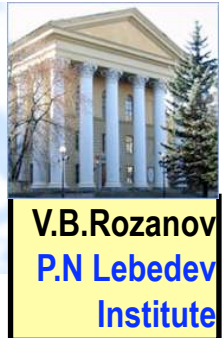


LIL experiments (3)

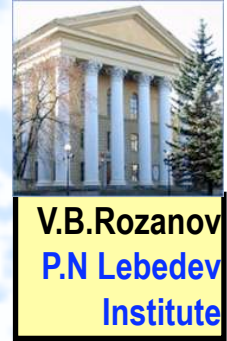


LIL experiments (4)

simulation by code CHIC-2D



LIL experiment simulation (1)



$$E_{\text{las}} \sim 10 \text{ kJ}, \quad \lambda = 0.351 \text{ } \mu\text{m}$$

$$\tau_{\text{las}} = 2.5 \text{ ns} \text{ at } 1/2q_{\text{max}}$$

$$q_{\text{las}} = 4 \cdot 10^{14} \text{ W/cm}^2$$

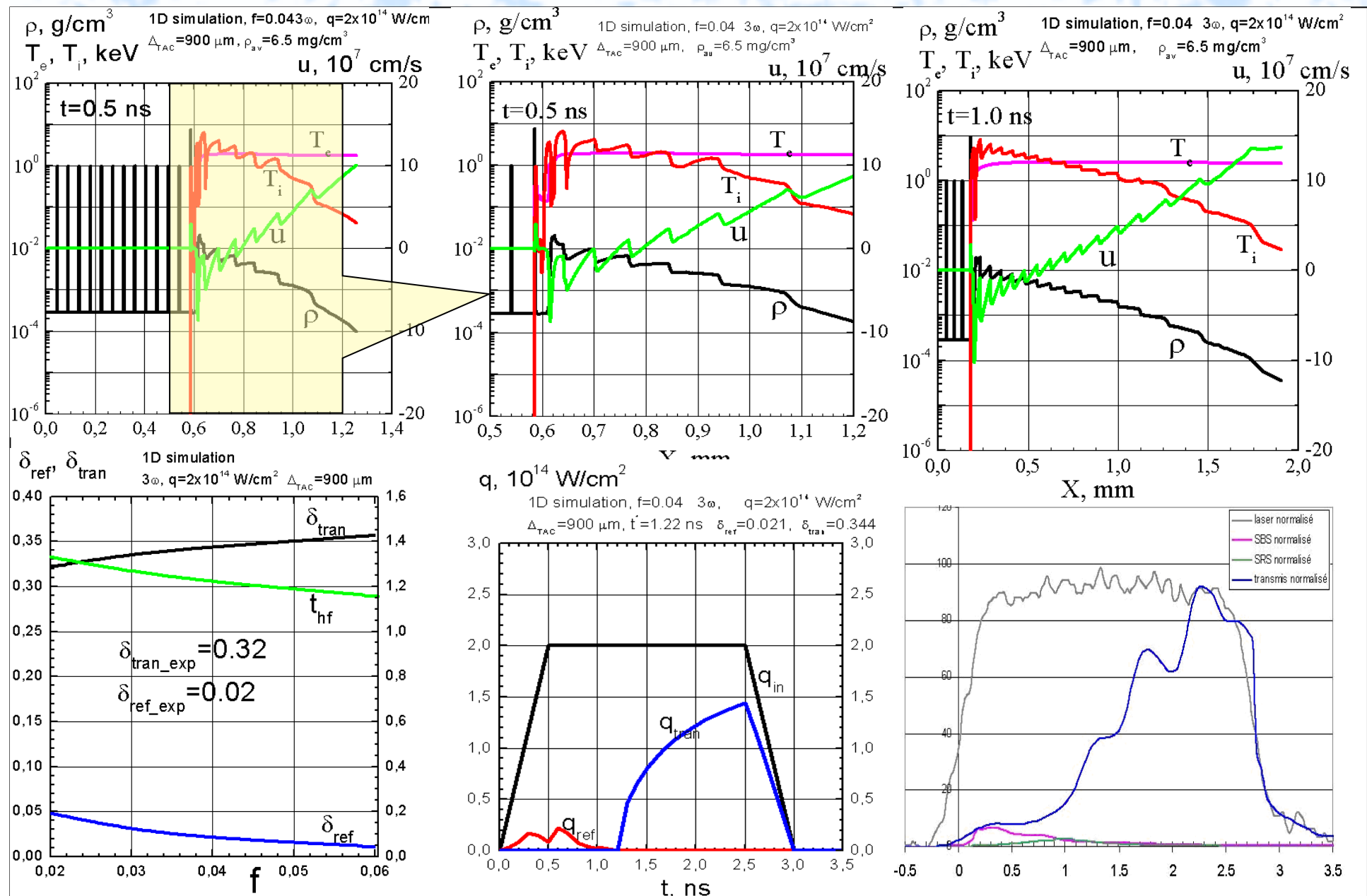
Target: **TAC-foam (900 μm)**

Foam density: **6.5 mg/cm³**

Simulation:

1D simulations were performed for incident laser flux $2 \times 10^{14} \text{ W/cm}^2$ because part of energy is lost due to transport in transverse direction.

LIL RAPID simulation (2)



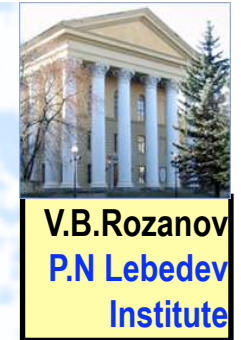
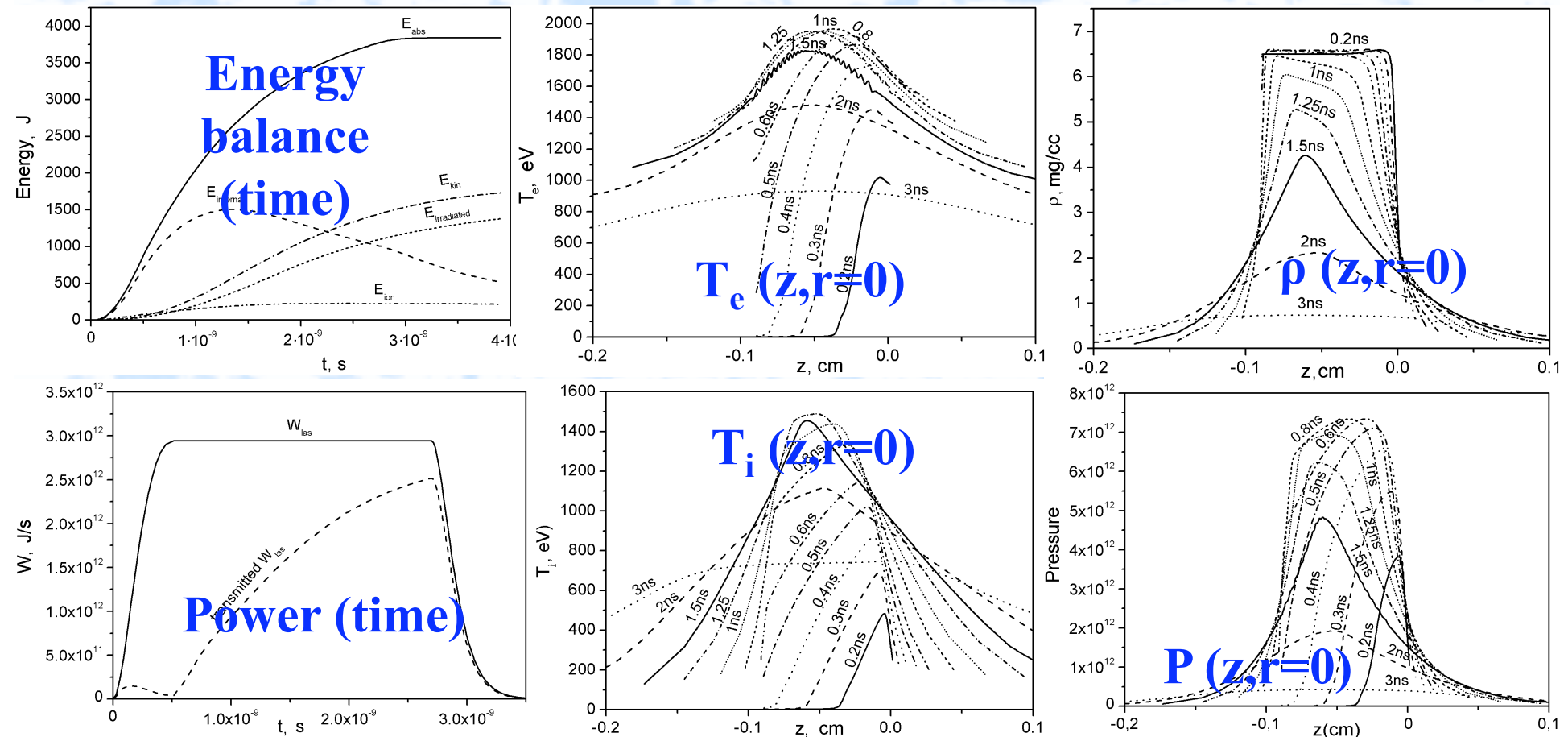
LIL experiment simulation(3)

2D LATRANT

ILP3: $E_{\text{las}} = 8 \text{ kJ}$, $\lambda = 0.351 \mu\text{m}$

$\tau_{\text{las}} = 2.7 \text{ ns}$ at $1/2q_{\max}$

Target: TMPTA ($\text{C}_{15}\text{H}_{20}\text{O}_6$)-foam, $900 \mu\text{m}$ Foam density: 6.5 mg/cm^3



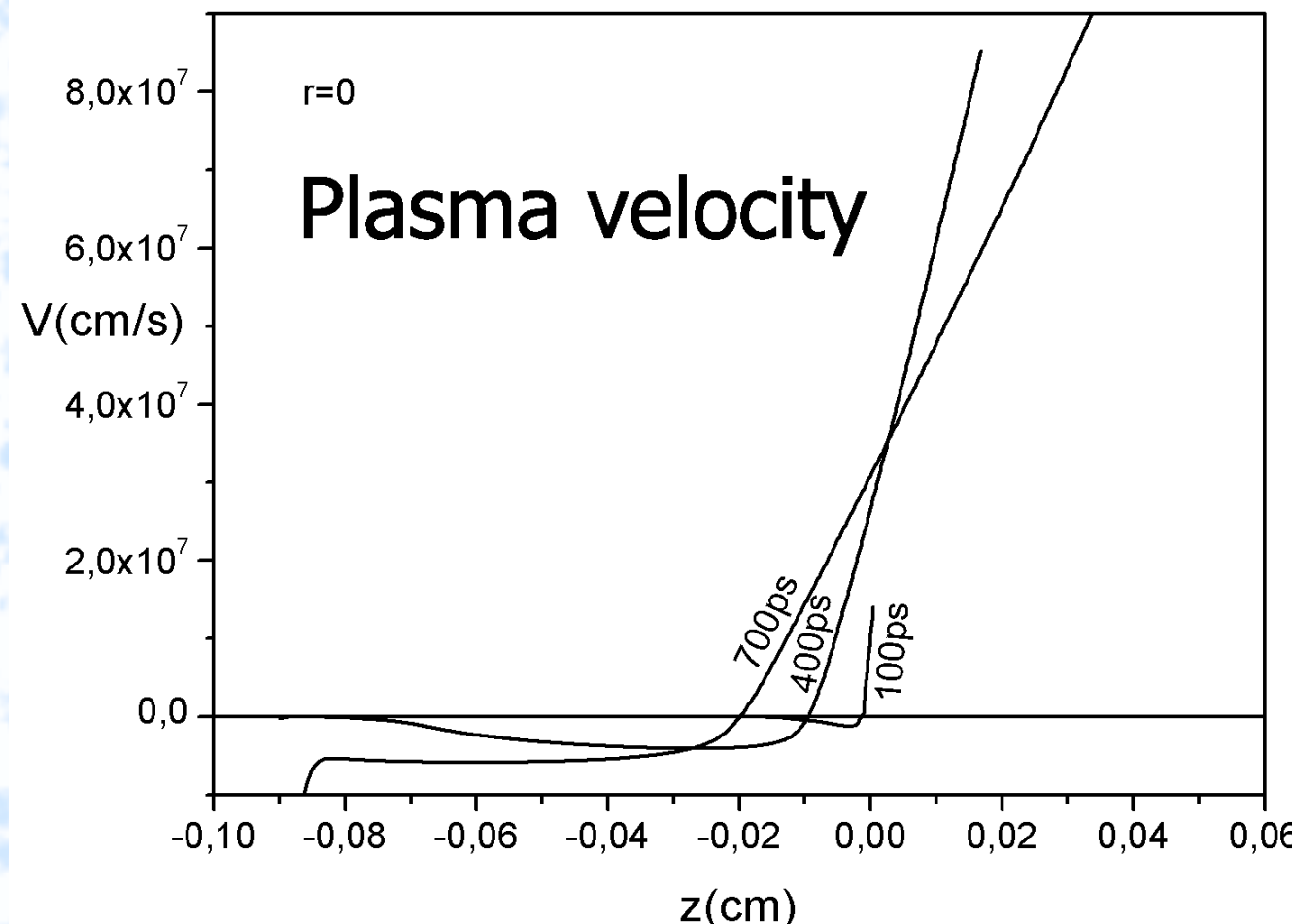
LIL experiment simulation⁽⁴⁾

2D LATRANT

ILP3: $E_{\text{las}} = 8 \text{ kJ}$, $\lambda = 0.351 \mu\text{m}$

$\tau_{\text{las}} = 2.7 \text{ ns}$ at $1/2q_{\text{max}}$

Target: TMPTA ($\text{C}_{15}\text{H}_{20}\text{O}_6$)-foam, $900 \mu\text{m}$ Foam density: 6.5 mg/cm^3

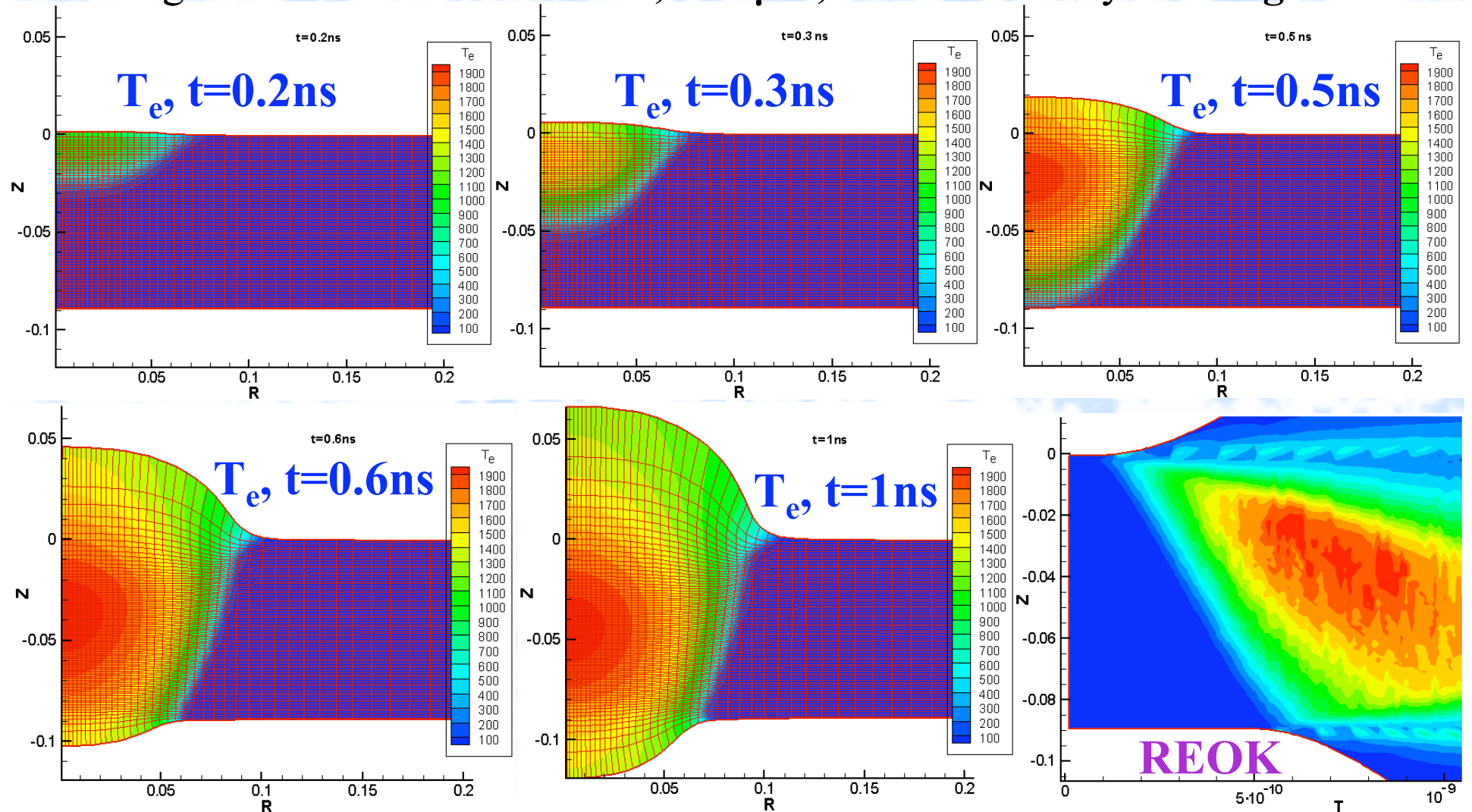


LIL experiment simulation(5)

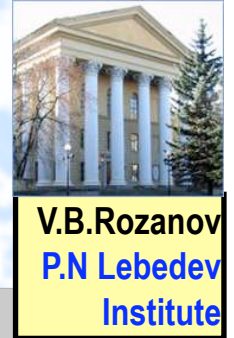
2D LATRANT



ILP3: $E_{\text{las}} = 8 \text{ kJ}$, $\lambda = 0.351 \mu\text{m}$ $\tau_{\text{las}} = 2.7 \text{ ns}$ at $1/2q_{\max}$
 Target: TMPTA-foam, $900 \mu\text{m}$, Foam density: 6.5 mg/cm^3



LIL: x-ray emissivity simulation in 2D LATRANT



TMPTA: Non-LTE integral emissivity

ρ , g/cm³

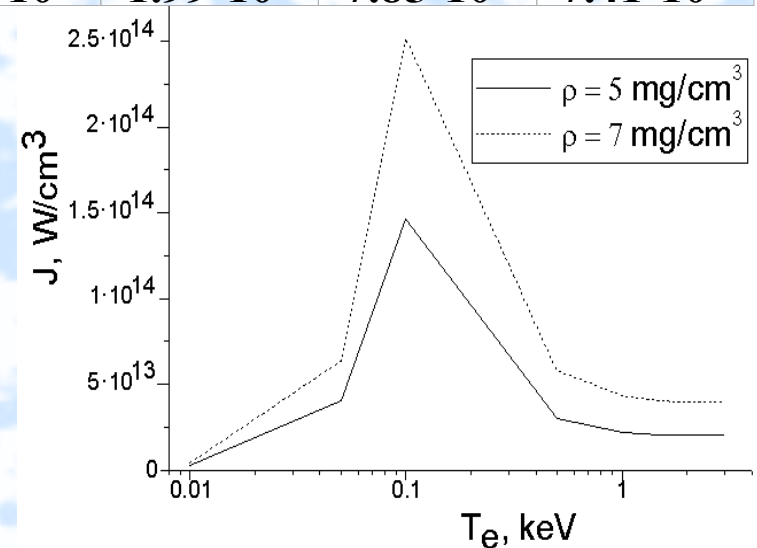
T_e , keV	0.005	0.007	0.010	0.015	0.030	0.050	0.100	1.000
0.01	$2.65 \cdot 10^{12}$	$3.98 \cdot 10^{12}$	$6.08 \cdot 10^{12}$	$9.46 \cdot 10^{12}$	$2.08 \cdot 10^{13}$	$3.85 \cdot 10^{13}$	$8.68 \cdot 10^{13}$	$2.67 \cdot 10^{15}$
0.05	$2.01 \cdot 10^{13}$	$3.63 \cdot 10^{13}$	$6.64 \cdot 10^{13}$	$1.27 \cdot 10^{14}$	$3.62 \cdot 10^{14}$	$7.37 \cdot 10^{14}$	$1.82 \cdot 10^{15}$	$3.18 \cdot 10^{16}$
0.10	$4.8 \cdot 10^{13}$	$9.31 \cdot 10^{13}$	$1.91 \cdot 10^{14}$	$4.17 \cdot 10^{14}$	$1.53 \cdot 10^{15}$	$3.76 \cdot 10^{15}$	$1.17 \cdot 10^{16}$	$2.29 \cdot 10^{17}$
0.50	$2.72 \cdot 10^{13}$	$5.37 \cdot 10^{13}$	$1.09 \cdot 10^{14}$	$2.43 \cdot 10^{14}$	$9.57 \cdot 10^{14}$	$2.6 \cdot 10^{15}$	10^{16}	$7.65 \cdot 10^{17}$
1.00	$2.18 \cdot 10^{13}$	$4.27 \cdot 10^{13}$	$8.67 \cdot 10^{13}$	$1.93 \cdot 10^{14}$	$7.6 \cdot 10^{14}$	$2.07 \cdot 10^{15}$	$8.07 \cdot 10^{15}$	$7.01 \cdot 10^{17}$
1.50	$2.11 \cdot 10^{13}$	$4.01 \cdot 10^{13}$	$8.14 \cdot 10^{13}$	$1.82 \cdot 10^{14}$	$7.18 \cdot 10^{14}$	$1.97 \cdot 10^{15}$	$7.7 \cdot 10^{15}$	$6.94 \cdot 10^{17}$
2.00	$2.07 \cdot 10^{13}$	$3.95 \cdot 10^{13}$	$8.04 \cdot 10^{13}$	$1.8 \cdot 10^{14}$	$7.11 \cdot 10^{14}$	$1.95 \cdot 10^{15}$	$7.68 \cdot 10^{15}$	$7.07 \cdot 10^{17}$
2.50	$2.04 \cdot 10^{13}$	$3.96 \cdot 10^{13}$	$8.06 \cdot 10^{13}$	$1.8 \cdot 10^{14}$	$7.14 \cdot 10^{14}$	$1.97 \cdot 10^{15}$	$7.76 \cdot 10^{15}$	$7.25 \cdot 10^{17}$
3.00	$2.05 \cdot 10^{13}$	$3.99 \cdot 10^{13}$	$8.11 \cdot 10^{13}$	$1.82 \cdot 10^{14}$	$7.21 \cdot 10^{14}$	$1.99 \cdot 10^{15}$	$7.85 \cdot 10^{15}$	$7.41 \cdot 10^{17}$

Balance: Theoretical estimation

$E_{abs} = 5.2 \text{ kJ} : 3.3 \text{ kJ}$ on heating + ionization $T_e=2\text{keV}$, $\rho=6.5\text{mg/cm}^3$, X-ray emission - 100J/ns

Where is energy?

2D simulation X-ray: **1.7kJ**



CONCLUSION



- Low and medium density laser plasma ($0.001\text{-}0.1 \text{ g/cm}^3$) with high Z admixture is the effective source of radiation in the spectral range $0.01\text{-}20 \text{ keV}$
- It was demonstrated, that
 - efficiency $>50\%$ for $h\nu \leq 2 \text{ keV}$
 - $1\text{-}3\%$ for $h\nu \approx 5\text{-}10 \text{ keV}$
 - 2% for $13.3 < \lambda < 13.7 \text{ nm}$
 - radiation energy $\approx 10 \text{ kJ}$ for $h\nu \leq 2 \text{ keV}$ (hohlraum situation $\sim 10^6 \text{ J}$)
 $100\text{-}500 \text{ J}$ for $h\nu \approx 5\text{-}10 \text{ keV}$
- $E_{\text{rad}}=10 \text{ kJ}$ corresponds to
 $\tau_L=1 \text{ ns}$ $N_\gamma=6 \cdot 10^{19} \quad h\nu \approx 1 \text{ keV}$
 $(4\pi)^{-1}(dN_\gamma/dt) \approx 5 \cdot 10^{27} (\text{s} \cdot \text{str})^{-1}$
- $E_{\text{rad}}=500 \text{ J}$ corresponds to
 $\tau_L=1 \text{ ns}$ $N_\gamma=3 \cdot 10^{17} \quad h\nu \approx 10 \text{ keV}$
 $(4\pi)^{-1}(dN_\gamma/dt) \approx 2 \cdot 10^{25} (\text{s} \cdot \text{str})^{-1}$
- These results open new possibilities in diagnostics, material and biomedical sciences, technology, X-ray laser physics.

References

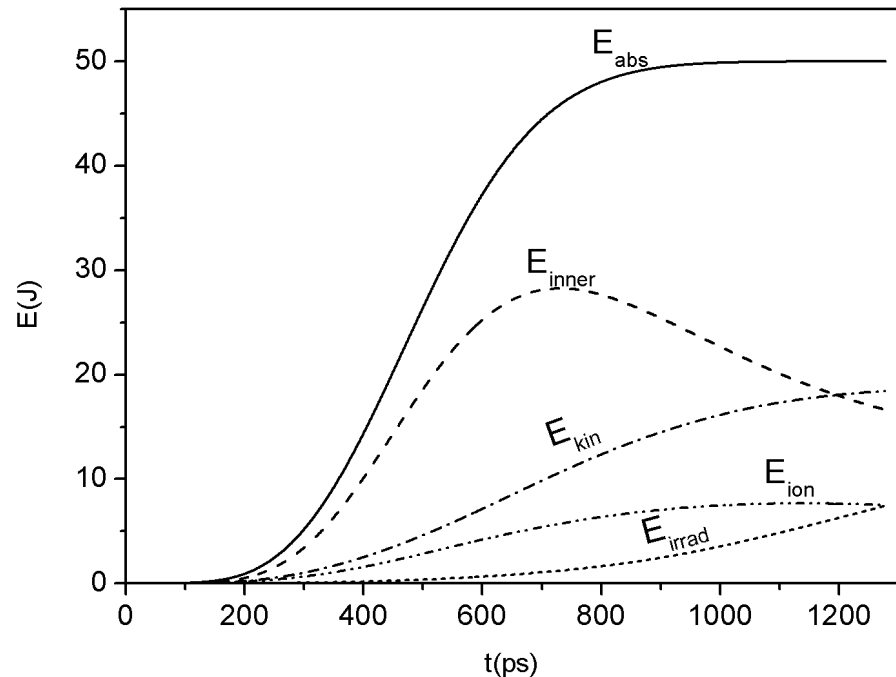
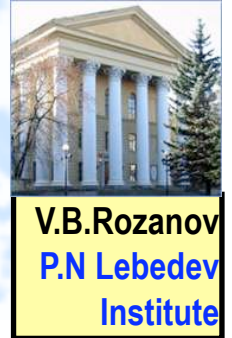


1. V. I. Annenkov, et al., Quantum Electronics, 35(11), 993, 2005.
2. S.Yu. Gus'kov, et al., Quantum Electronics, 33(2), 95, 2003.
3. S.Yu. Gus'kov, et al., Proc. of SPIE, 4424, 332-335, 340-347, 2001.
4. S.Yu. Gus'kov, et al., JETP, 81(2), 296, 1995.
5. V. B. Rozanov. Physics-Uspekhi, 47(4), 359, 2004.
6. V. F. Tishkin, et al., Math. Modeling, 7(5), 15, 1995 (in Russian).
7. LLE Review, 102, 67, 2005
8. I. G. Lebo, et al., Las. Part. Beams, 22(3), 267, 2004.
9. V. Rozanov, et al., J. Phys.: Conf. Ser., 112, 022010, 2008

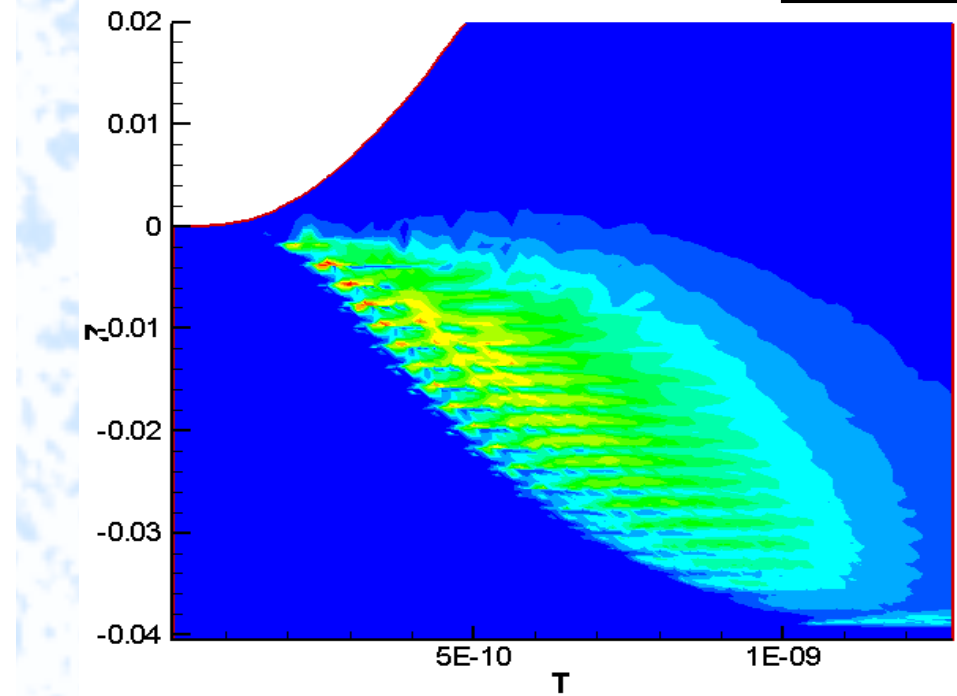
This work was supported by the joint grant of Russian Foundation of Basic Research and Japan Society for the Promotion of Science (# 06-02-91226-JF).

PALS Numerical simulations (1)

**TAC 4.5 mg/cm³, 1 ω , 50 J,
LATRANT code, 20 layers, r=0**



Energy balance

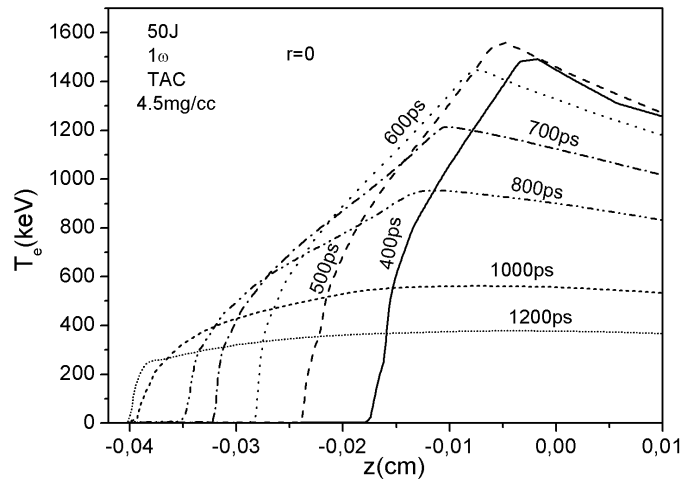
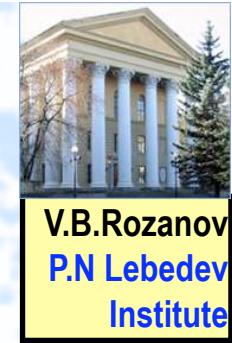


REOK data

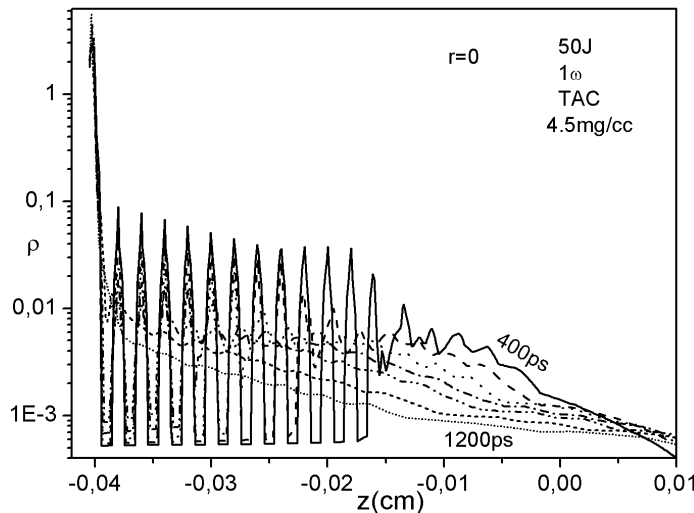
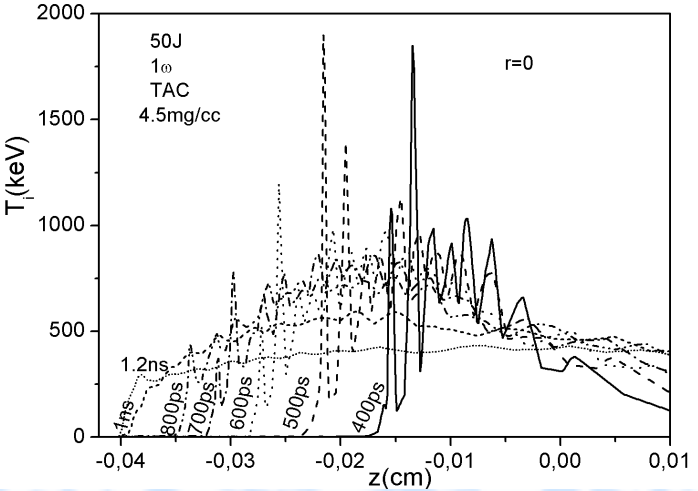
LATRANT takes into account radiation transport in multigroup approach and gas dynamics according to an improved Lagrangian difference scheme (E.N.Aristova, A.B.Iskakov. LATRANT: two-dimensional radiative Lagrangian gas dynamics for ICF problems, Matematicheskoe modelirovaniye, v. 16 (2004), №3, p.63-77

PALS Numerical simulations (2)

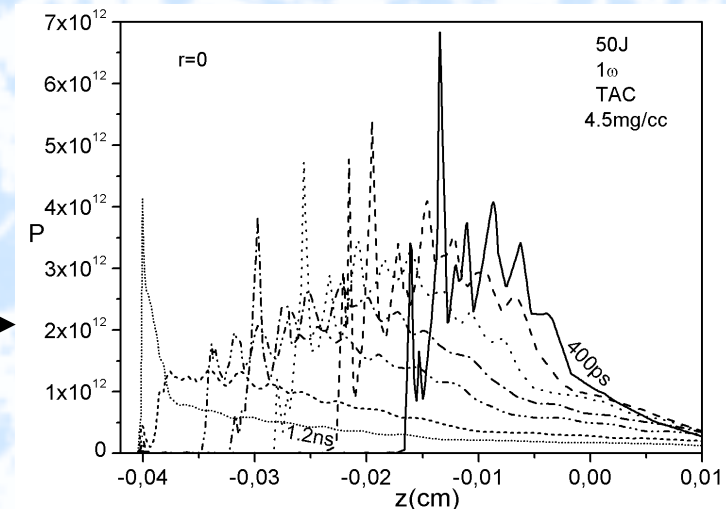
TAC 4.5 mg/cm³, 1 ω , 50 J, 20 layers, r=0



Electron
Ion
temperatures



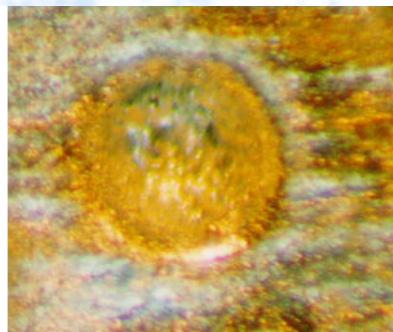
Density
Pressure



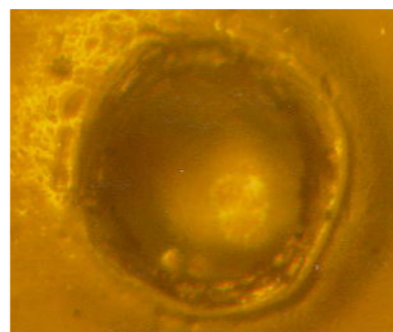


Debris problem

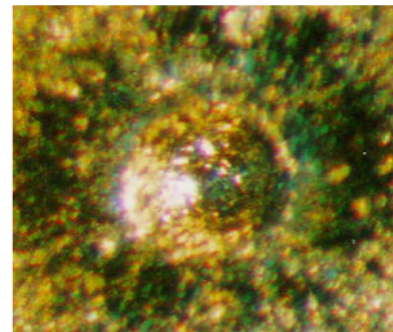
Al



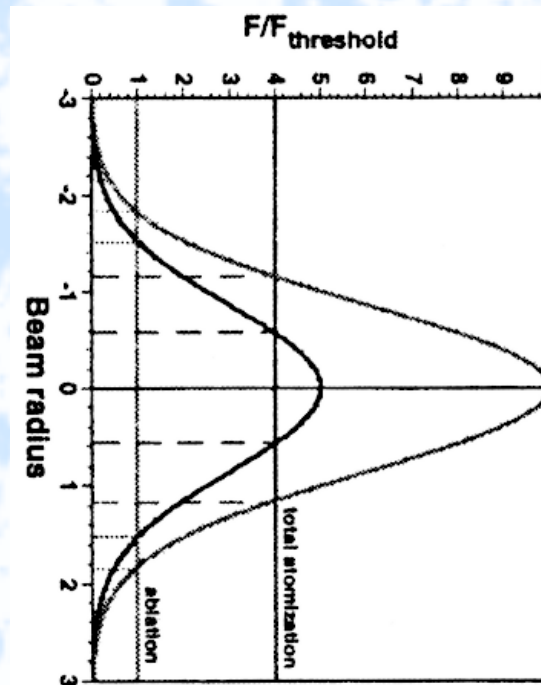
$(CH)_n$



Ti



200 mkm



Atomization/
ablation
thresholds for
short laser pulse
(E.G.Gamaly et
al, 2004)

Experimental results for
 $E_L=4-20\text{ J}$, $R_L=100\mu\text{m}$, $\tau=1\text{ ns}$
(LPI, "Kanal" facility, 2001)